UC Berkeley
UC Berkeley Previously Published Works

Title
Improving the prediction of African savanna vegetation variables using time series of MODIS products

Permalink
https://escholarship.org/uc/item/6qk0s5s2

Authors
Tsalyuk, Miriam
Kelly, Maggi
Getz, Wayne M

Publication Date
2017-09-01

DOI
10.1016/j.isprsjprs.2017.07.012

Peer reviewed

eScholarship.org Powered by the California Digital Library
University of California

ISPRS Journal of Photogrammetry and Remote Sensing 131 (2017) 77–91

Contents lists available at ScienceDirect

ISPRS Journal of Photogrammetry and Remote Sensing

journal homepage: www.elsevier.com/locate/isprsjprs

Improving the prediction of African savanna vegetation variables using time series of MODIS products

Miriam Tsalyuk [a,*], Maggi Kelly [a], Wayne M. Getz [a,b]

[a] Department of Environmental Sciences, Policy & Management, 130 Mulford Hall #3114, University of California Berkeley, CA 94720-3114, USA
[b] School of Mathematical Sciences, University of KwaZulu-Natal, Private Bag X54001, Durban 4000, South Africa

ARTICLE INFO

Article history:
Received 16 February 2017
Received in revised form 11 July 2017
Accepted 28 July 2017

Keywords:
Vegetation cover
Enhanced Vegetation Index (EVI)
Leaf Area Index (LAI)
Fraction of Photosynthetically Active Radiation (FPAR)
Partial Least Square Regression (PLSR)
Model transferability

ABSTRACT

African savanna vegetation is subject to extensive degradation as a result of rapid climate and land use change. To better understand these changes detailed assessment of vegetation structure is needed across an extensive spatial scale and at a fine temporal resolution. Applying remote sensing techniques to savanna vegetation is challenging due to sparse cover, high background soil signal, and difficulty to differentiate between spectral signals of bare soil and dry vegetation. In this paper, we attempt to resolve these challenges by analyzing time series of four MODIS Vegetation Products (VPs): Normalized Difference Vegetation Index (NDVI), Enhanced Vegetation Index (EVI), Leaf Area Index (LAI), and Fraction of Photosynthetically Active Radiation (FPAR) for Etosha National Park, a semiarid savanna in north-central Namibia. We create models to predict the density, cover, and biomass of the main savanna vegetation forms: grass, shrubs, and trees. To calibrate remote sensing data we developed an extensive and relatively rapid field methodology and measured herbaceous and woody vegetation during both the dry and wet seasons. We compared the efficacy of the four MODIS-derived VPs in predicting vegetation field measured variables. We then compared the optimal time span of VP time series to predict ground-measured vegetation. We found that Multiyear Partial Least Square Regression (PLSR) models were superior to single year or single date models. Our results show that NDVI-based PLSR models yield robust prediction of tree density ($R^2 = 0.79$, relative Root Mean Square Error, rRMSE = 1.9%) and tree cover ($R^2 = 0.78$, rRMSE = 0.3%). EVI provided the best model for shrub density ($R^2 = 0.82$) and shrub cover ($R^2 = 0.83$), but was only marginally superior over models based on other VPs. FPAR was the best predictor of vegetation biomass of trees ($R^2 = 0.76$), shrubs ($R^2 = 0.83$), and grass ($R^2 = 0.91$). Finally, we addressed an enduring challenge in the remote sensing of semiarid vegetation by examining the transferability of predictive models through space and time. Our results show that models created in the wetter part of Etosha could accurately predict trees' and shrubs' variables in the drier part of the reserve and vice versa. Moreover, our results demonstrate that models created for vegetation variables in the dry season of 2011 could be successfully applied to predict vegetation in the wet season of 2012. We conclude that extensive field data combined with multiyear time series of MODIS vegetation products can produce robust predictive models for multiple vegetation forms in the African savanna. These methods advance the monitoring of savanna vegetation dynamics and contribute to improved management and conservation of these valuable ecosystems.

© 2017 International Society for Photogrammetry and Remote Sensing, Inc. (ISPRS). Published by Elsevier B.V. All rights reserved.

1. Introduction

Savanna ecosystems cover about fifth of the Earth's land surface and just under half of Africa's land area (Ciais et al., 2011; Shackleton and Scholes, 2011). These ecosystems provide pivotal ecosystem services including carbon sequestration, water filtration, soil stability, meat and dairy production, fuel wood provision, tourism, and recreation (Solbrig, 1996; Vågen et al., 2005). In addition, African savannas harbor rich biodiversity and provide habitat and connectivity for far-roaming wildlife (Sankaran et al., 2013).

Abbreviations: AVHRR, advanced very high resolution radiometer; DPM, Disc Pasture Meter; EVI, Enhanced Vegetation Index; FPAR, Fraction of Photosynthetically Active Radiation; GIS, geographic information systems; LAI, Leaf Area Index; MODIS, Moderate Resolution Imaging Spectroradiometer; NDVI, Normalized Difference Vegetation Index; NIR, near infrared; NPP, Net Primary Productivity; PCQ, point-centered quarter method; PLSR, Partial Least Square Regression; QC, quality control; RMSEP, Root Mean Squared Error of Prediction; rRMSE, relative Root Mean Square Error; SPOT, Satellite Pour l'Observation de la Terre (Satellite for observation of Earth); SWIR, shortwave infrared; VI, vegetation index; VP, vegetation product.

* Corresponding author.
E-mail addresses: miri.tsa@gmail.com (M. Tsalyuk), maggi@berkeley.edu (M. Kelly), wgetz@berkeley.edu (W.M. Getz).

http://dx.doi.org/10.1016/j.isprsjprs.2017.07.012
0924-2716/© 2017 International Society for Photogrammetry and Remote Sensing, Inc. (ISPRS). Published by Elsevier B.V. All rights reserved.

However, savanna ecosystems face degradation due to changes in land use, climate change, fire, and management regimes (Mathieu et al., 2009; Mitchard and Flintrop, 2013; Vogel and Strohbach, 2009). Monitoring rapid changes in savannas requires a method that maintains sufficiently high temporal resolution over large spatial extents. Remote sensing is a viable tool to predict biophysical measurements of cover, density, and biomass of savanna vegetation (Ban et al., 2015; Boschetti et al., 2013; Choudhury, 1992; Dube and Mutanga, 2015; Naidoo et al., 2012; Rahimzadeh-Bajgiran et al., 2012; Zhu and Liu, 2015). For convenience, we use the term "prediction" hereafter to refer to the modeled relationship between reflectance data and field-based vegetation measurements.

Savannas are extensive, and often remote and inaccessible, complicating protocols for their monitoring. Field methodologies for measuring vegetation change are typically limited in extent, expensive, and time consuming. Therefore, the use of low and moderate resolution remote sensing, including Moderate Resolution Imaging Spectroradiometer (MODIS), has been applied to characterize savanna vegetation throughout Africa (Eisfelder et al., 2012). Nonetheless, the sparse vegetation in these arid and semi-arid areas and high reflectance of soil background continue to present a major challenge to the use of remote sensing to predict continuous vegetation variables (Ali et al., 2016; Ghulam et al., 2007; Rahimzadeh-Bajgiran et al., 2012; Svoray et al., 2013). Moreover, savanna vegetation is senesced during prolonged periods of the year (Eisfelder et al., 2012). Low chlorophyll content of senescent vegetation reduces the red-to-near infrared (NIR) spectral contrast, which impairs our ability to distinguish vegetation from background soil. These characteristics present additional challenges when using remote sensing to directly predict dry biomass (Homer et al., 2013; Huete, 1988; Mayr and Samimi, 2015; Meyer and Okin, 2015). One approach to addressing these challenges is to use spectral products targeted at enhancing vegetation that use red, near infrared (NIR), and shortwave infrared (SWIR) wavelengths which are particularly sensitive to vegetation changes (Houborg et al., 2007).

MODIS provides four preprocessed vegetation products. Two of these products are vegetation indices, Normalized Difference Vegetation Index (NDVI), and Enhanced Vegetation Index (EVI). The other two are vegetation quantities derived partly from spectral vegetation indices: Leaf Area Index (LAI), and Fraction of Photosynthetically Active Radiation (FPAR) (Knyazikhin et al., 1999). We refer to these four MODIS-derived products as "Vegetation Products" (VPs). These MODIS VPs are freely available, atmospherically and geometrically corrected, and based on extensive field validation campaigns (Solano et al., 2010). Therefore, these VPs are readily available to practitioners, and particularly valuable for savanna conservation applications (Li et al., 2015a; Tsalyuk et al., 2015).

NDVI has been widely applied to predict vegetation cover, above-ground biomass and greenness (Jacquin et al., 2010). While the relationship between NDVI and above-ground green biomass is well established (Eisfelder et al., 2012; Li et al., 2012; Zhu and Liu, 2015), research has indicated the limited capacity of NDVI to predict senesced vegetation (Xu et al., 2014). Conversely, the EVI index is sensitive to a wider range of canopy cover than NDVI (Huete et al., 2002). The EVI index includes the red and IR bands of NDVI, and additionally incorporates a blue band, soil adjustment factor, and atmospheric resistance terms, which correct the influence of aerosol on the red band (Sjostrom et al., 2011). This correction is specifically useful in open canopies such as savanna and shrublands, where the background signal may have prominent effect on radiometric measurements of vegetation (Huete et al., 2002). There is a strong correlation between EVI and gross primary productivity (GPP) in African ecosystem (Jin et al., 2013; Sjostrom et al., 2011). Li et al. (2012) show a strong relationship between EVI, Net Primary Productivity (NPP), and forage production in rangelands. Time series of MODIS EVI was successfully used to classify land cover in Northern China (Zhang Xia et al., 2008), identify maize crop cultivation areas (Zhang et al., 2014), and monitor global crop yield (Zhang and Zhang, 2016).

Leaf Area Index (LAI) provides information on plant canopy structure by measuring the total green leaf area per unit ground-surface area (Lotsch et al., 2003). FPAR is a unitless fraction, measuring the proportion of radiation absorbed by the canopy out of the total available radiation in the photosynthetically active wavelengths of the spectrum 400–700 nm. FPAR is an important measure of carbon cycling and energy budget (Huete et al., 2002). Both LAI and FPAR have been measured in the field as prominent indicators of vegetation condition. Research has demonstrated that both these vegetation properties have higher correlations with senesced grass biomass than does NDVI (Asner et al., 1998; Butterfield and Malmstrom, 2009). FPAR was shown to correlate with both green grass biomass and litter canopy, indicating its ability to predict dry vegetation biomass (Machwitz et al., 2015). Recently, LAI and FPAR have being used as satellite-derived products for calculating surface photosynthesis, evapotranspiration, land cover, and net primary productivity (Huete et al., 2002; Knyazikhin et al., 1999; LP DAAC, 2002-2012; Myneni et al., 2002).

The MODIS-based algorithm of LAI/FPAR products was designed to use up to seven spectral bands of MODIS surface reflectance (648, 858, 470, 555, 1240, and 2130 nm) (Knyazikhin et al., 1998). However, until recently only the red (648 nm) and infrared bands (858 nm) were used (Yan et al., 2016), similar to NDVI. The relationships among NDVI and LAI and NDVI and FPAR have received attention (Myneni et al., 2010). However, these relationships are influenced by land cover and the vegetation canopy structure (Lotsch et al., 2003). To deal with this, MODIS LAI/FPAR algorithm uses NDVI bands and relies on world classification of six biomes together with extensive field validation to define vegetation structure (Lotsch et al., 2003). The algorithm links surface bi-directional reflectance factor (BRT) to structural and spectral properties of vegetation and soil (Yan et al., 2016). Importantly, LAI/FPAR in situ measurements show a good correlation with MODIS-derived values (Fensholt et al., 2004; Zhao et al., 2007).

An additional challenge in applying remote sensing in savannas is encompassing the high inter- and intra-annual variability of the vegetation in these ecosystems. Capturing seasonal and inter-annual variation is especially important in savannas, where vegetation biomass is highly dependent on variable rainfall (Scanlon et al., 2005). Time series of VPs capture vegetation phenology over time; and, therefore, they can improve the prediction of vegetation variables (Rao et al., 2015; van Hoek et al., 2016; Zhu and Liu, 2015). Indeed, integrated (summed) values and maximum annual NDVI and FPAR values over the growth year show strong correlations with above-ground herbaceous biomass (Li et al., 2015a; Zhang et al., 2016). Annually integrated VI data show better correlations with field measured herbaceous biomass than a single-date VI value (Verbesselt et al., 2006; Yi et al., 2008; Zhou et al., 2013). Time series information, such as times of green up and senescence/dormancy onset and the length of the growing season have been used to describe vegetation phenology (Lu et al., 2014a, 2014b; Zhang et al., 2003), and to differentiate between growing cycles of trees or grasses (Archibald and Scholes, 2007). Time series of MODIS-derived EVI predict maize (Zhang et al., 2014) and winter wheat (Qiu et al., 2017) cultivated areas across China with considerable accuracy.

In spite these recent developments, remote sensing of biophysical variables of savanna vegetation remains a challenge (Mayr and Samimi, 2015; Meyer and Okin, 2015). A major hindrance in the application of remote sensing data for monitoring and management is transferability of models between sites, when trying to apply models developed for one area to predict vegetation variables in others (Cutler et al., 2012; Foody et al., 2003; Sumnall et al., 2016). Eisfelder et al. (2012) identified the transferability of remote sensing-based methods to measure biomass as a major challenge in semi-arid environments. The high spatial and temporal variability in savanna vegetation present a challenge to transfer established relationships between ground-based measurements and satellite information.

The aim of this study is to improve the application of remote sensing to predict vegetation in an African savanna in Etosha National Park, Namibia. We examine to what degree incorporating time series data of four Vegetation Products (VPs) derived from MODIS improves the prediction of vegetation biophysical variables in a savanna ecosystem. We compare the ability of these VPs to predict the cover, density, and biomass of different savanna vegetation forms (grass, shrub, and trees), and assess the accuracy of each product's predictions. We hypothesize that since each VP has unique radiometric and analytical properties, each will be best suited to predict a specific vegetation variable. Finally, our study addresses the challenge of transferring remote sensing-based models across space and time by using extensive field data, multiyear satellite information, and using Partial Least Square Regression (PLSR) to carry out robust statistical modeling. Our goals are to:

1. Create reliable and accurate remote sensing models to predict density, cover, and biomass, of the three main vegetation forms in savanna ecosystems: trees, shrubs, and grasses;
2. Use time series of MODIS VPs to predict vegetation and quantify the improvements in prediction models with extended time periods;
3. Compare four MODIS-derived VPs – NDVI, EVI, LAI, and FPAR – in terms of their ability to predict accurately different vegetation form; and
4. Assess the transferability of our vegetation predictive models across space and time.

2. Methods

2.1. Study site

Etosha National park is a 22,270 km^2 reserve, located in north-central Namibia (18°45′S, 15°30′E) (Fig. 1). It is a semi-arid savanna with a gradient of 200–450 mm of rainfall per year. Etosha experiences three main seasons: cold-dry (May–August), warm-dry (September–December), and warm-wet (January–April) season (Du Plessis et al., 1998). Etosha is primarily flat, transitioning to hillier terrain in its far west. The main vegetation types in the reserve are grassland savanna, steppe, shrubland, Mopani (*Colophospermum mopane*) tree savanna, and a mix trees savanna (Du Plessis, 2001; Le Roux et al., 1988). Etosha pan is a natural saline lake depression spanning 4410 km^2, which is dry most of the year and is seasonally filled with water (de Beer et al., 2006).

2.2. Vegetation measurement

We collected extensive vegetation data across Etosha over two field seasons. During the dry season, June to August 2011, we measured 348 sites. The dry season is the suggested time for field validation of remote sensing data, since then the differences between the vegetation types are most pronounced (McCoy, 2005). During the wet season of March to April 2012, we resampled 110 out of the original 348 sites. We performed wet season sampling to evaluate seasonal differences in vegetation measurements, and to evaluate how well remote sensing-based models developed for one season can be applied to predict vegetation in the other.

Sampling sites were at least 500 m away from each other to minimize spatial correlation. We sampled at least 50 m away from roads and at least 1 km away from watering points to minimize sampling of possible edge effects of these features. To avoid off-road driving, we sampled within a strip of 50–300 m away from roads. Within this buffer, we used stratified random sampling design to ensure equal representation of each vegetation class in Etosha. We stratified the region based on physiognomic vegetation classification derived from Landsat 5 TM that was created for Etosha in 1996 (Sannier et al., 1996; Taylor et al., 1996). These vegetation classes are described in Table 1 and presented in Fig. 2. Based on Sennier's classification map, we choose sampling sites located within at least 1 km^2 of uniform vegetation class, to insure sampling within uniform 250 × 250 m MODIS pixels.

One of our goals was to create an efficient, accurate, and relatively rapid method for field sampling of vegetation in the vast landscapes savannas encompass. We compared and calibrated visual estimation with detailed field measurements. To avoid bias,

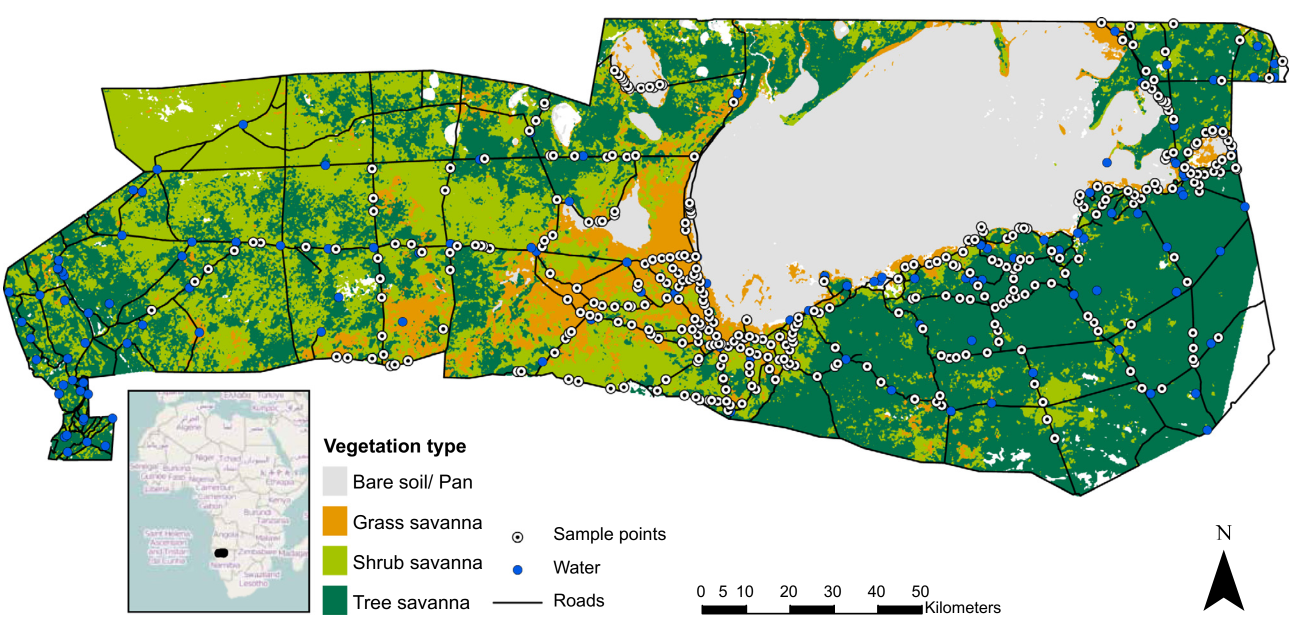

Fig. 1. Map of the study area, Etosha National Park, Namibia. The locations of sampling sites (stars) and watering points (circles) are marked.

Table 1
Vegetation classes.

Class name	% Tree cover	% Shrub cover	% Dwarfed shrubs	Plant height (m)
Bare soil	–	–	–	–
Grassland	–	–	<1%	–
Steppe	<1%	<1%	>1%	<0.5
Grass savanna	1–5%	1–5%	<1%	–
Shrub savanna	<5%	>5%	–	0.5–2
Low tree savanna	>5%	–	–	2–5
High tree savanna	>5%	–	–	>5

Adapted from Du Plessis (1999).

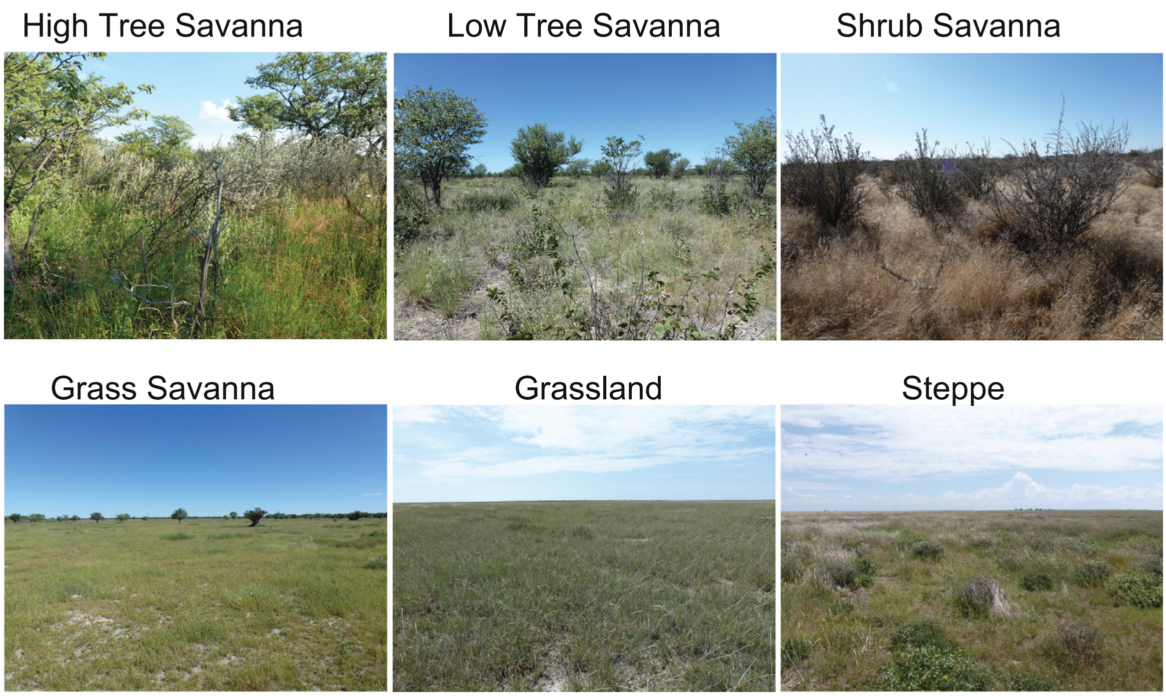

Fig. 2. Six main physiognomic vegetation classes in Etosha, based on Sannier et al. (1996).

all visual estimations were performed by the same observer. We compared the physiognomic vegetation class to visual cover estimation of bare soil, grass, shrubs, and trees. We then calibrated all visual estimations with field measurements of cover. Table 2 summarizes all vegetation variables and their measurement methods.

2.2.1. Woody vegetation measurements

We used the plotless point-centered quarter (PCQ) method to measure woody vegetation. PCQ is an accurate and labor efficient method for vegetation measurement that does not assume plants are randomly distributed (Engeman et al., 1994; White et al., 2008). At each site, we picked a random central sampling point around which we divided the area into four equal quarters. In each quarter we measured the two shrubs and the two trees closest to the central point, to obtain a set of eight distance values R_1 to R_8 (eight trees and eight shrubs in total). We measured the distance from the central point to the trunk, the canopy area, height, and the diameter at breast height (DBH, 1.37 m) of each individual plant. The species of each measured plant was recorder. Tree density D (trees per hectare) at each sampling site was calculated using the following equation (Pollard, 1971) in terms of a correction factor (CF) and the eight distances R_1 to R_8:

$$D = \frac{28 * \mathrm{CF} * 10^4}{\pi * \sum_{i=1}^{8} R_i^2} \quad (1)$$

CF accounts for the proportion of missing individuals in each point (Warde and Petranka, 1981). The factor 10^4 converts density measurement from plants per square meter to plants per hectare. Same calculations were used to calculate shrub density.

Canopy cover C (m^2/ha) was calculated for each sampling site as the average of eight measured canopy sizes multiplied by the density. Woody biomass B (in metric tons) at each sampling site was calculated, separately for trees and for shrubs, using the following equation formulated by Henry et al. (2011) in terms of trunk radius r_i, tree height h_i, and tree density D (as determined by Eq. (1)):

$$B = \sum_{i=1}^{8} \frac{(\pi r_i^2 * h_i * 0.5 * 0.7 * 10^3)D}{8} \quad (2)$$

We used average woody specific gravity = 0.7 Mg m^{-3} as suggested for Etosha (Alleaume et al., 2005), and average coefficient = 0.5 for conic trees suggested by Henry et al. (2011).

2.2.2. Grass measurements

We used a 1×1 m frame to measure herbaceous vegetation. We recorded percent cover of grass, soil, and forbs within the frame and identified the two dominant grass species and their cover. We used two complementary methods to measure grass biomass: assigning a visual biomass class of 1–7 (C) for each 1 m^2 frame, and measuring the height h (cm) of a Disc Pasture Meter (DPM) (Trollope and Potgieter, 1986). We calibrated both

Table 2
Summary of the vegetation field measurements.

Vegetation form	Variable	Visual estimation	Measurement method	Comments
	Vegetation class	Visual estimation	Calculation using measured cover of grass, shrubs, and trees	Dominant vegetation species recorded
Grass	Cover	–	Percent cover in 1 m^2 square	–
	Biomass	Biomass class 1–7 visual estimation	Disc Pasture Meter (height)	Both methods calibrated by clipping and weighting dry biomass in 75 plots
Shrub	Density	–	PCQ[a]	Eq. (1)
	Cover	V	Canopy size × density	–
	Biomass	–	Canopy size × height × diameter × density	Eq. (2)
Tree	Density	–	PCQ	Eq. (1)
	Cover	V	Canopy size × density	–
	Biomass	–	Canopy size × height × diameter × density	Eq. (2)

[a] PCQ = point-centered quarter method.

methods by clipping and weighting dry biomass grass in a subsample of 75 points. Calibration of grass biomass showed strong, significant correlations between DPM measurements and direct biomass weighting ($R^2 = 0.94$, $p < 0.001$, $n = 75$); and between visual class estimation C and field grass measurement ($R^2 = 0.87$, $p < 0.001$). We determined the grass biomass B_{total} (g/m^2) at each sampling site by averaging the two methods over five measurements taken at each site.

2.3. MODIS vegetation products

For each vegetation form: grasses, shrubs, and trees, we compared models based on MODIS Vegetation Product (VP) that would best correlate with its field measurements of cover, density, and biomass (eight field variables in total). We used four MODIS-derived VPs: MODIS MOD13Q1 provides Normalized Difference Vegetation Index (NDVI) and Enhanced Vegetation Index (EVI); MODIS MOD15A2 provides Leaf Area Index (LAI) and Fraction of Photosynthetically Active Radiation (FPAR) (Table 3). We acquired MODIS data products for 2006–2012, collection 5, from NASA's Reverb website (EODIS, 2013). We extracted the values of each VP in the pixel overlaying each sampling site, using the Spatial Analyst Tools in ArcGIS 10.2 (ESRI, 2011).

MODIS images the earth daily. MOD13Q1 product for NDVI/EVI provides data as a 16-days average in a 250 × 250 m resolution, while MOD15A2 product for LAI/FPAR provides 8-day average with a 1 × 1 km resolution (Table 3). There is limited cloud cover over Etosha National park year round, providing good quality control (QC) values in most pixels, as indicated by the products' QC layers; we also removed null values (249–255). Marginal quality pixels occurred within the Etosha pan; therefore, we excluded this region from the analysis. Pixel gaps in the MODIS dataset were removed from the analyses to avoid introducing error that may result from the application of various extrapolation or smoothing methods (Weiss et al., 2014). We resampled FPAR and LAI data to match NDVI's 250 × 250 m resolution using nearest neighbor assignment resampling technique through the application of the "Conditional" function in Spatial Analysis tools of ArcGIS 10.2 in batch mode (ESRI, 2011). Table 3 summarizes the products used.

NDVI is calculated in terms of ρ_{red} and, ρ_{NIR}, which are the reflectance measured by the satellite sensor in the red (620–670 nm) and near infrared (841–876 nm) wavelengths, respectively, using Eq. (3) (Tucker et al., 1981):

$$\mathrm{NDVI} = \frac{\rho_{NIR} - \rho_{red}}{\rho_{NIR} + \rho_{red}} \tag{3}$$

In addition to the red and the NIR wavelengths used above, EVI includes an atmospheric resistance term by adding ρ_{blue} which is the reflectance measure at the blue wavelength (459–479 nm). Addition of canopy background adjustment L, and aerosol correction factors C_1 and C_2, correct the blue and red bands relative to the NIR band. The correction and adjustment factors used in the MODIS EVI algorithm are: $L = 1$, $C_1 = 6$ and $C_2 = 7.5$, using Eq. (4) (Huete et al., 2002):

$$\mathrm{EVI} = \frac{\rho_{NIR} - \rho_{red}}{\rho_{NIR} + C_1\rho_{red} - C_2\rho_{blue} + L} \tag{4}$$

The MODIS-based LAI/FPAR products currently use only the red (648 nm) and IR bands (858 nm) of MODIS (Yan et al., 2016). The algorithm then uses one of six biomes for each location to solve a radiative transfer equation to estimate LAI and FPAR values. LAI values range from 0 to 10 and FPAR ranges from 0 to 1 (Knyazikhin et al., 1999; Myneni et al., 2002).

2.4. Statistical analysis

2.4.1. Summary statistics

We used six years of MODIS VPs data (October 2006 to October 2012) to incorporate inter- and intra-annual variations into our vegetation predictive models. Inspecting time series patterns of each VP revealed that there is one annual growth cycle in Etosha. The annual minimum values of all four VPs occur in the hot-dry

Table 3
Moderate Resolution Imaging Spectroradiometer (MODIS) vegetation products used in this research and the parameters of each product.

Vegetation product	MODIS product	Temporal resolution	Spatial resolution	Boolean dates/years used	Data range	Scale factor
NDVI	MOD13Q1	16-days	250 × 250 m	289/2006–273/2012	−2000, 10,000 Fill value: −3000	0.0001
EVI	MOD13Q1	16-days	250 × 250 m	289/2006–273/2012	−2000, 10,000 Fill value: −3000	0.0001
FPAR	MOD15A2	8-days	1 × 1 km	289/2006–281/2012	0–100 Null values: 249–255	0.01
LAI	MOD15A2	8-days	1 × 1 km	289/2006–281/2012	0–100 Null values: 249–255	0.1

season, around mid-October. Therefore, we used "growth year" for all the analyses, calculating one year from October 16th of the previous year to October 15th of the current year. For each year and each VP, we calculated summary statistics for all MODIS data points provided for one year, 23 data points per year for NDVI/EVI, or 46 points for LAI/FPAR. We calculated the following nine summary statistics values: annual minimum; annual maximum; annual median; annual sum defined as: $\mathrm{sum}_{\mathrm{vp}} = \sum_{i=1}^{n}\mathrm{VP}_i$, where i is each date the VP is calculated by MODIS ($n = 23$ for NDVI/EVI, or $n = 46$ for LAI/FPAR); annual average calculated as: $\overline{\mathrm{VP}_{\mathrm{vp}}} = \frac{1}{n}\cdot\sum_{i=1}^{n}\mathrm{VP}_i$; and annual standard deviation calculated as: $\mathrm{SD}_{\mathrm{vp}} = \sqrt{\frac{1}{n-1}\cdot\sum_{i=1}^{n}(\mathrm{VP}_i - \overline{\mathrm{VP}}_i)^2}$. Additionally, we identified the Julian date of annual minimum occurrence and date of annual maximum occurrence. The length of the growing season was calculated as the number of consecutive days that VP values were above the 50th percentile for that year. We multiplied value by 8 or 16, to match MOD15A2 or MOD13Q1 time intervals, respectively. Finally, for each sampling point we extracted the VP values at the closest date to the field sampling.

As a baseline analysis, we performed univariate regressions between each of the eight vegetation variables (density, cover, and biomass of grasses, shrubs, and trees) and a single VP value, calculated for the closest date to vegetation measurement in the field. We also calculated the correlation between each variable and each of the four VPs summary statistics for one year, 2011, the year when the primary field sampling took place.

2.4.2. Partial Least Square Regression (PLSR)

To create predictive models that incorporate up to six years of VP data while reducing the dimensionality of the data, we used Partial Least Square Regression (PLSR) (Darvishzadeh et al., 2011; Hansen and Schjoerring, 2003; Huang et al., 2004). PLSR is a powerful regression technique that is able to handle datasets with multiple predictor variables that exhibit high levels of multicollinearity. The method generates orthogonal latent variables (components) that are linear combinations of the standardized predictor variables, such that each component explains the maximum covariance between the response and the predictor variables (Mevik and Wehrens, 2007). The loadings are the regression coefficients, or relative weights, of each of the original predictor variables in the new component (Asner and Martin, 2008; Hansen and Schjoerring, 2003; Mitchell et al., 2012; Ramoelo et al., 2013; Schmidtlein and Sassin, 2004). PLSR is a good collinearity reduction technique for time series analysis, and was successfully used with multitemporal MODIS data (Lazaridis et al., 2011). Woody vegetation measurements (shrubs and trees) appeared to be log-normally distributed; therefore, we used the natural log of these measurements as the response variable (Wold et al., 2001). For grass and shrub measurements, we performed analysis using only sample points at open cover types (grassland, grass savanna, steppe, and shrub savanna). We performed these analyses using package *pls* in R (Mevik and Wehrens, 2007).

To validate the statistical robustness of PLSR models, we performed leave-one-out cross-validation and used the resulting root-mean-squared error of prediction (RMSEP) as a measure of model quality (Mevik and Cederkvist, 2004). This method is regarded as the best estimation of error and model quality for PLSR, while avoiding over-fitting the model (Lazaridis et al., 2011; Mevik and Cederkvist, 2004). We used the exponents of RMSEP values for log models.

To choose the optimal number of PLSR components we plotted the leave-one-out cross-validation RMSE as a function of the number of components for every combination of vegetation variable (density, cover, and biomass of grass, shrubs, and trees) and Vegetation Product (NDVI, EVI, LAI, FPAR) (Supplemental materials Fig. S1). We chose to use the first ten PLSR components because this number minimized the model error (RMSE) while optimizing the percent of variance explained (equivalent to R^2) for all vegetation variables (Darvishzadeh et al., 2008; Geladi and Kowalski, 1986). We used the same number of components (10) for all the models, to be able to compare between them.

2.4.3. Time series analysis

We hypothesized that including time series of remote sensing data will encompass the temporal variability and phenological patterns of savanna vegetation, and therefore will better predict vegetation variables. To test this hypothesis, we compared the relationship between VP-based models and each vegetation variable at three time scales: (1) one VP date, closest to date of field sampling, (2) summary statistics of one year of VP, and (3) multi-year VP data of two to six years. We assumed that a period of few years would incorporate average annual rainfall fluctuations that affect vegetation growth. We performed cross validation of the models by randomly separating the data 50–50, to test and prediction datasets, and assessed how well each model predicted the data, as estimated by R^2 and RMSEP. We further performed continues analysis comparing models that incorporated one, two, and up to six years of VP data. We compared models quality using their R^2 and RMSEP.

2.4.4. Comparing MODIS vegetation product (VPs)

We compared the ability of each VP to predict each vegetation form (grasses, shrubs, tress), and their measurements (cover, density, and biomass). For each vegetation form, we constructed separate PLSR prediction model, based on one of the four VPs (32 models total). For each vegetation variable, we compared four multivariate PLSR models, based on one of the four VPs. We assessed the quality and robustness of the model that each VP produced using four methods: First, to provide a more intuitive measure of error, we calculated percent error as Relative Root Mean Squared Error (rRMSE), by dividing the RMSEP of each model by the average value of the vegetation variable (Song et al., 2013). Second, we compared which of the four VP-based models has the highest R^2. We calculated the relative ability of each VP to predict each vegetation variable as: $\Delta R_i^2 = (R_i^2 - R_{max}^2)/R_{max}^2$, where i is one of the four VP-based models, and $R_{\max}^2$ is the R^2 of the best model among the four. Third, we compare the VPs by plotting the R^2 and RMSEP for the first 25 PLSR model components, of each of the four models, and assessing the number of components needed in each model to reach higher R^2 with the lowest model error. Finally, we assessed the models' quality by cross validation: we trained the model on two-thirds of the data (randomly selected) testing it on the remaining one-third, and examining the RMSE of the predicted values. We compared the resulting predicted versus measured values and their RMSEP.

2.5. Transferability

We assessed whether our models could be transferred across space and time by applying a predictive model built using a training dataset to predict vegetation variables of a test dataset. The ability to transfer vegetation prediction models across space and time is also a strong measure of models' robustness and an indication that the variables were not over-fitted (Sumnall et al., 2016). We compared the RMSEP of predicted versus measured vegetation variables. We examined model transferability in *space* by dividing Etosha to a drier area, where the annual rainfall was below the reserve's ten-year annual rainfall average (360 mm/year), and a wetter area. This roughly separated Etosha into the east versus the central/west parts of the reserve. We then applied predictive models trained using field sites from the wetter area to predict vegetation variables in the dried area, and vice versa. This analysis also examined whether precipitation had an effect on models' prediction quality.

We examined model transferability in *time*, by applying models trained using field measurements from the dry season of 2011 to predict vegetation measured in the wet season of 2012.

3. Results

3.1. Using MODIS to predict vegetation variables

Univariate regressions of vegetation variables on MODIS-VPs provided weak but significant predictions. (Please see Supplementary Tables S1–S12 for complete results of univariate models.) When we used only one VP date, from the date closest to field measurement, NDVI was the best predictor, with R^2 ten-fold or more than the other three VPs. NDVI annual average was the best predictor of grass cover ($R^2 = 0.43$, $p < 0.001$), shrub cover ($R^2 = 0.3$, $p < 0.00$), tree density, tree cover ($R^2 = 0.34$, $p < 0.001$), and tree biomass ($R^2 = 0.37$, $p < 0.001$) (S1–S12).

Univariate regressions with VP summary statistics of one year (2011) improved the results (Fig. 3). Here, again, NDVI gave better predictive models than the other VPs for tree density ($R^2 = 0.44$, $p < 0.001$), cover ($R^2 = 0.42$, $p < 0.001$), and biomass ($R^2 = 0.37$, $p < 0.001$) (S9–S12).

Partial Least Square Regression (PLSR) significantly improved the models' ability to predict measured vegetation variables. PLSR models using first 10 components predicted up to 84% of variability in grass cover (RMSEP = 30% cover), and 91% of variability in grass biomass, but with high error margins (RMSEP = 47 g/m^2) (Table 4).

Using NDVI, LAI, and FPAR-based PLSR models we achieved robust prediction of shrub density and shrub cover (82–83% variance explained with <1% error, RMSEP = 11 shrubs/ha for EVI model). All VPs produced similar quality prediction of shrub biomass (83% of variability explained), but the error was high (rRMSE = 15%) (Table 5).

NDVI PLSR model produced good prediction of tree density (79% variability explained, RMSEP = 4.3 trees/ha). NDVI and FPAR gave similarly good prediction of tree canopy cover (79% variability, RMSEP = 4.3 m^2/ha). FPAR produced good model for tree biomass (76% variability, RMSEP = 0.89%) (Table 6).

3.2. Optimal time span for predicting vegetation variables

We assessed the contribution of integrating VP data over time to model prediction quality, comparing the predicted versus measured values of models built for three different time spans (Fig. 3, Tables 4–6 and S1–S12). Summary statistics VP values for one year (2011) gave 30% better predictions of vegetation variables than VP acquired at a single date. For example, NDVI-based model for tree density had $R^2 = 0.54$ between measured and predicted values when using NDVI data of one year (mean of 23 biweekly NDVI data points), whereas NDVI at one date produced $R^2 = 0.41$ ($p < 0.001$). Furthermore, the PLSR model using six years of NDVI data provided considerable improvement (110%) in prediction of tree density ($R^2 = 0.89$) (Fig. 3).

The quality of PLSR prediction models continued to improve when adding from one up to six years of VP data to the analysis (Fig. 4). Percent variance explained (R^2) increased by about 40% over the range, for both tree and grass cover, while there was little to no increase in the error (Fig. 4).

Both the time span and the timing (date) of VP values used in the PLSR models affected the quality of the predictions. While these results varied across different vegetation variables, we observed the following common patterns. VP values from the rainy season (January–March) and the maximum annual VP values had the largest loadings on the PLSR components (Fig. 5). Interestingly, rainy season values from two or three years prior to the field measurement had the highest model coefficients (Fig. 5).

3.3. Comparing MODIS vegetation products (VPs)

We compared four PLSR models for each vegetation variable, where each model was based on one of the four VPs. Each vegetation form had a different VP that gave its best prediction (Table 7). However, often the differences between the VPs were not pronounced (Tables 4–6, Supplemental materials Fig. S1). In most cases, EVI was a good predictor of vegetation cover, while FPAR was the best predictor of biomass (Tables 4–7).

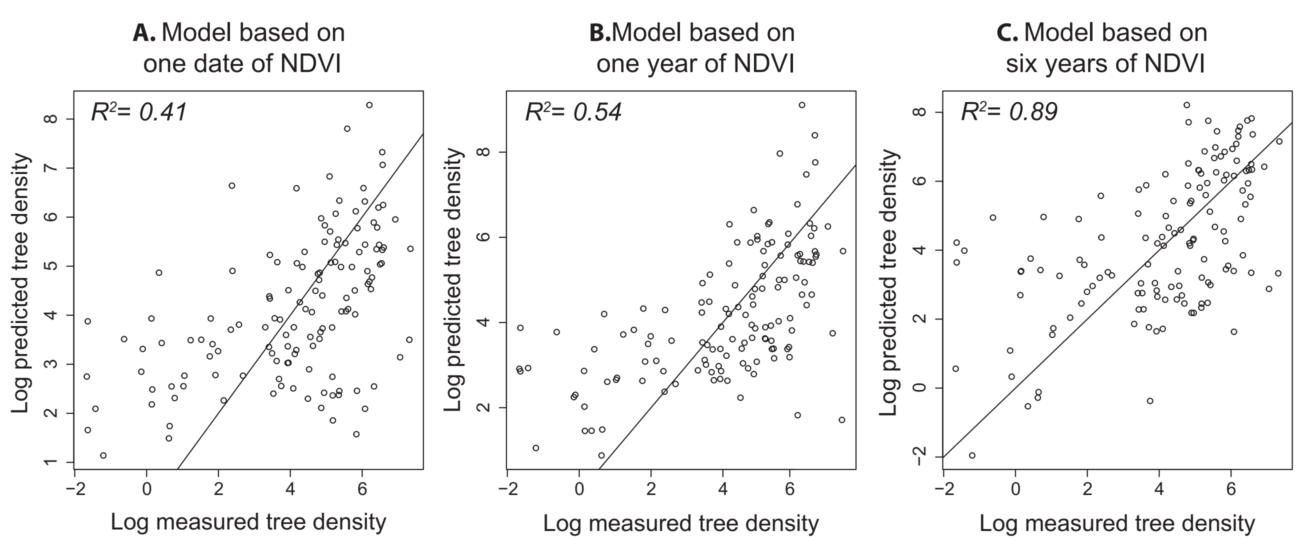

Fig. 3. Model predicted versus field measured log values of tree density from predictive models based on NDVI data in three different time spans. Diagonal lines have an aspect ratio of 1. n = 310. A. One NDVI value, closest date to field measurement. B. Average annual NDVI for 2011, based on an average of 23 values (each value is a 16-day composite). C. PLSR model based on six years of NDVI data. Note that R^2 values in this figure are somewhat higher than the results for the overall model, since the models presented here were created using a training dataset of 50% of the data selected at random.

Table 4
Results of partial least square regression for grass variables.

MODIS product	Variable	RMSEP[a]	rRMSE[b] (percent error)	R^2	ΔR^2	RMSEP random[c]	RMSEP wet to dry[d]	RMSEP dry to wet[e]	RMSEP 2012[f]	RMSEP 2011–2012[g]
NDVI	Grass cover	30	55.41	83	−1	27	*24*	*26*	21	25
EVI	Grass cover	30	55.17	*84*	–	32	30	34	23	27
LAI	Grass cover	*24*	*43.69*	82	−3	*25*	25	29	*16*	*24*
FPAR	Grass cover	24	44.16	82	−2	31	27	26	17	24
NDVI	Grass biomass	57.69	58.96	90	−1	66.01	69.44	64.61	115.57	172.68
EVI	Grass biomass	60.68	62.01	84	−7	*48.6*	77.62	81.36	155.19	161.86
LAI	Grass biomass	50.99	52.11	90	−1	53.5	55.29	66.39	88.83	176.22
FPAR	Grass biomass	*47.15*	*48.18*	*91*	–	50.03	*55.29*	*61.54*	*86.42*	*181.68*

Best results marked in italics.
[a] RMSEP – Root Mean Square Error of Prediction. RMSEP units are percent cover and gram/m^2, for grass cover and grass biomass, respectively.
[b] rRMSE – Relative root mean square error. ΔR^2 – percent difference in R^2 relative to R^2 of the best model.
[c] RMSEP of a model built with random two-thirds of the data and tested on the remained third.
[d] RMSEP of model trained with data from the wet areas and tested in the dry areas.
[e] RMSEP of models trained with data from the dry areas and tested in the wet areas.
[f] RMSEP of models built for 2012 wet season data.
[g] RMSEP for models trained with data from the dry season of 2011 and tested in the wet seasons of 2012.

Table 5
Results of partial least square regression for shrub variables.

MODIS product	Variable	RMSEP[a]	rRMSE[b] (percent error)	R^2	ΔR^2	RMSEP random[c]	RMSEP wet to dry[d]	RMSEP dry to wet[e]	RMSEP 2012[f]	RMSEP 2011–2012[g]
NDVI	Shrub density	*8.83*	*0.24*	81	−2	*9.52*	14.19	12.34	18.48	13.07
EVI	Shrub density	11.51	0.32	*82*	–	20.96	19.14	24.44	34.96	14.15
LAI	Shrub density	11.28	0.31	81	−1	14.58	11.17	12.30	13.10	*8.22*
FPAR	Shrub density	9.63	0.27	81	−1	11.01	*9.24*	*9.83*	*11.86*	8.47
NDVI	Shrub cover	*9.72*	*0.75*	80	−4	10.88	20.80	15.09	16.32	8.02
EVI	Shrub cover	10.58	0.82	*83*	–	*8.93*	24.85	15.31	19.75	7.65
LAI	Shrub cover	11.73	0.91	83	0	13.29	11.67	12.26	*8.14*	*6.13*
FPAR	Shrub cover	10.56	0.82	83	0	11.76	*10.62*	*11.72*	8.48	6.15
NDVI	Shrub biomass	11.53	15.62	82	−2	18.49	19.00	23.89	18.92	8.21
EVI	Shrub biomass	12.19	16.52	*83*	–	*10.55*	35.30	16.38	33.76	8.64
LAI	Shrub biomass	15.37	20.82	82	−2	22.97	*12.39*	15.53	*10.40*	8.36
FPAR	Shrub biomass	*11.38*	*15.41*	83	−1	12.09	12.86	*15.14*	12.46	*8.00*

Best results marked in italics.
[a] RMSEP – Root Mean Square Error of Prediction. RMSEP units are shrubs/hectare, m^2/ha, and metric tons, for shrub density, cover, and biomass, respectively.
[b] rRMSE – Relative root mean square error. ΔR^2 – percent difference in R^2 relative to R^2 of the best model.
[c] RMSEP of a model built with random two-thirds of the data and tested on the remained third.
[d] RMSEP of model trained with data from the wet areas and tested in the dry areas.
[e] RMSEP of models trained with data from the dry areas and tested in the wet areas.
[f] RMSEP of models built for 2012 wet season data.
[g] RMSEP for models trained with data from the dry season of 2011 and tested in the wet seasons of 2012.

Grass cover was best predicted by an EVI-based model, since it explained the highest proportion of the variance (R^2 = 84%). However, LAI/FPAR showed lower, but still high, model error for grass cover (rRMSE = 43% vs. 55%). For grass biomass, FPAR gave a strong prediction of R^2 = 91, but the error was high (rRMSE = 48%) (Table 4).

Shrub density, cover, and biomass, were best modeled with EVI, but the difference from the other VPs was small (1–2%). FPAR and EVI produced similar predictions of shrub biomass (R^2 = 0.83), though FPAR had a smaller error (rRSME = 15%) (Table 5).

Tree density was best predicted by NDVI, with 3–7% higher R^2 than the other models. Tree canopy was predicted equally well by FPAR and NDVI; the latter had slightly smaller error. Tree biomass was best predicted by FPAR (R^2 = 0.76). These results were very close (1%) to the NDVI model, which also produced lowest error (Table 6).

3.4. Model transferability

We examined model transferability in space and time: in other words, how well did a VP-based model created in one region predict vegetation in a different region or in another season. Based on the models selected for each vegetation variable (Tables 4–6), we used NDVI to assess transferability of models for tree variables and FPAR to assess transferability models for grass variables.

3.4.1. Transferability in space

When applying a model built with field data from the wetter area of Etosha to predict tree variables in the drier area, we achieved good correlation between predicted and measured values of tree density (RMSE = 8.51 trees/ha), cover (RMSE = 6.42 m^2/ha), and biomass (RMSE = 11.74 trees/ha) (Fig. 6A, Table 6). There were also good correlations between predicted and measured tree values for models created for the drier part of Etosha and applied in the wetter part (RMSE = 7.57 trees/ha). Generally, there was a good fit between predicted and measured values for all tree variables, and particularly for tree biomass. A few values in the higher range of tree density were overestimates (Fig. 6B).

For grass cover and biomass, prediction models trained for the wet area of Etosha overestimated measures in the drier area (RMSEP = 24% cover) (Fig. 7A). Transferring models from drier to wetter area produced slightly better fit (Fig. 7B). All RMSE values were quite high, around 50%. For all vegetation forms, the error was generally lower for models created the dry part of Etosha

Table 6
Results of partial least square regression for trees variables.

MODIS product	Variable	RMSEP[a]	rRMSE[b] (percent error)	R^2	ΔR^2	RMSEP random[c]	RMSEP wet to dry[d]	RMSEP dry to wet[e]	RMSEP 2012[f]	RMSEP 2011–2012[g]
NDVI	Tree density	*4.30*	*1.98*	*79*	–	*4.78*	*8.51*	7.57	*5.05*	2.98
EVI	Tree density	5.17	2.39	75	−5	6.15	11.34	*6.14*	7.86	*2.95*
LAI	Tree density	7.62	3.52	73	−7	7.95	12.56	12.81	6.31	3.90
FPAR	Tree density	6.37	2.94	76	−3	7.02	12.50	14.94	7.12	3.83
NDVI	Tree cover	*4.34*	*0.30*	78	−1	*5.06*	*6.42*	8.83	6.76	3.00
EVI	Tree cover	5.02	0.35	74	−5	6.52	10.12	*5.87*	7.06	*2.82*
LAI	Tree cover	6.79	0.47	77	−1	6.80	8.38	10.05	*6.06*	3.89
FPAR	Tree cover	5.67	0.39	*78*	–	5.34	8.49	10.31	7.42	4.01
NDVI	Tree biomass	*8.08*	*0.62*	75	−1	9.74	*11.74*	*13.07*	10.39	4.20
EVI	Tree biomass	9.23	0.71	73	−4	*8.10*	15.52	15.52	*7.68*	*3.76*
LAI	Tree biomass	13.54	1.04	73	−4	16.84	20.55	30.00	9.25	5.13
FPAR	Tree biomass	11.63	0.89	*76*	–	11.48	16.95	22.63	12.14	5.78

Best results marked in italics.
[a] RMSEP – Root Mean Square Error of Prediction. RMSEP units are trees/hectare, m^2/ha, and metric tons, for tree density, cover, and biomass, respectively.
[b] rRMSE – Relative root mean square error. ΔR^2 – percent difference in R^2 relative to R^2 of the best model.
[c] RMSEP of a model built with random two-thirds of the data and tested on the remained third.
[d] RMSEP of model trained with data from the wet areas and tested in the dry areas.
[e] RMSEP of models trained with data from the dry areas and tested in the wet areas.
[f] RMSEP of models built for 2012 wet season data.
[g] RMSEP for models trained with data from the dry season of 2011 and tested in the wet seasons of 2012.

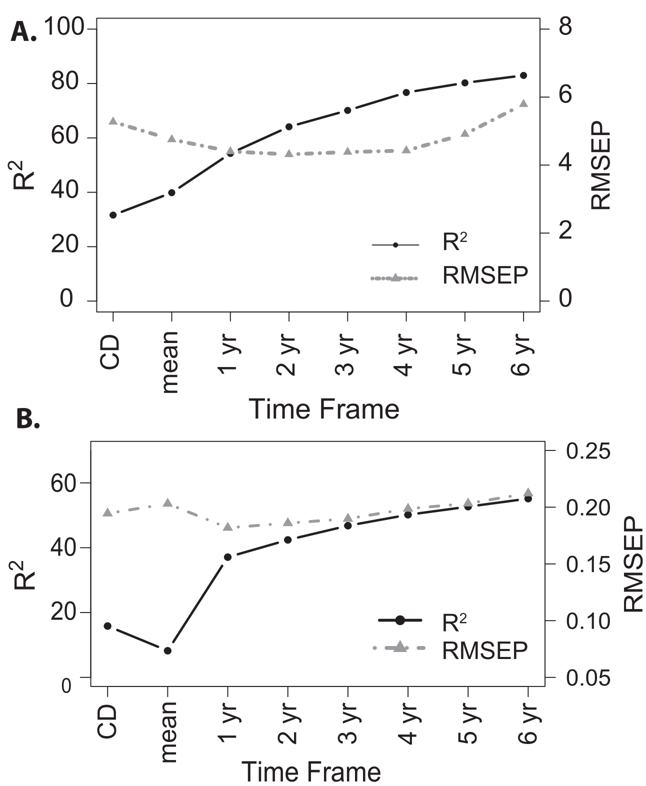

Fig. 4. Model prediction quality as a function of length of time series used to fit the model. A. NDVI model for tree canopy cover (m^2/ha). B. NDVI model for grass cover (%). CD = NDVI at the closest date to field measurement. Mean = NDVI annual average of the year of field measurement (2011).

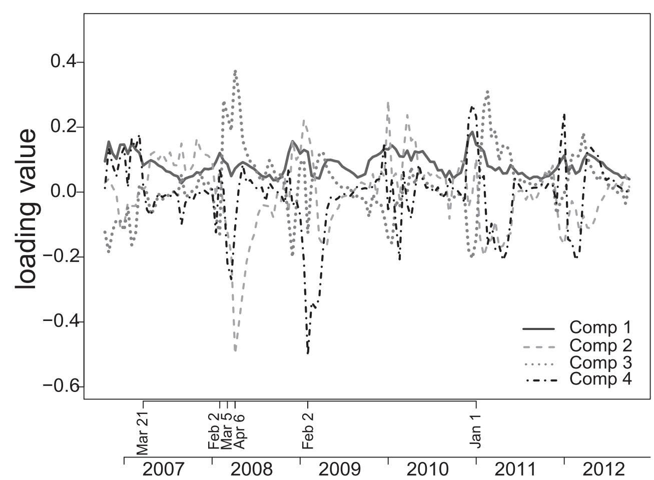

Fig. 5. Loadings on the first four components of NDVI time series Partial Least Square Regression (PLSR) model to predict tree density. Each line denotes one component. Variables with the highest loadings are marked on the horizontal-axis.

Table 7
Summary of best MODIS vegetation product (VP) to predict each vegetation variables.

Vegetation form	Variable	MODIS vegetation product[a]
Grass	Cover	EVI
	Biomass	FPAR
Shrubs	Density	EVI
	Cover	FPAR
	Biomass	FPAR
Trees	Density	NDVI
	Cover	NDVI
	Biomass	FPAR

[a] Best VP for PLSR model selected by highest R^2 and lowest error.

and transferred to predict data in the wet part, than the other way around (Tables 4–6).

3.4.2. Transferability in time

We achieved good model transferability in time: models that were built using field data from the dry season of 2011 gave robust predictions of tree density, canopy cover, and biomass in the wet season of the following year, 2012 (Fig. 6C). The RMSEPs were <1% for temporal transferability of models for shrubs and trees (Tables 5 and 6). The models created for grass in the dry season overestimated grass cover but underestimated grass biomass in the wet season (Fig. 7C).

3.5. Vegetation maps

Using the best PLSR model for each vegetation form (see Section 3.2) we created a series of maps to predict each vegetation variable for Etosha National Park. Fig. 8 is one example of percent tree cover for Etosha, based on the NDVI PLSR model.

4. Discussion

The prediction of vegetation variables using remote sensing is challenging in savanna ecosystems due to low vegetation cover, high background signal, soil reflectance, and senesced vegetation. Variability in space and time hinders the transferability of remote sensing models to other regions. Creating accurate and transferable predictive models is further challenged by limited availability of field data and by the reflectance properties of savanna ecosystems. In this paper, we addressed these challenges by combining four key components: (1) developing methodology for extensive field sampling, (2) using time series data to account for vegetation temporal variability, (3) comparing between four MODIS-derived VPs that contain different radiometric information, (4) creating vegetation prediction models that are transferable through space and time, hence demonstrating that these methods are robust.

4.1. Field sampling methodology

Measuring vegetation for remote sensing validation in savanna ecosystems is often challenging and time consuming due to the vast landscapes and limited accessibility to these areas. In this research, we demonstrate an extensive and relatively rapid field methodology to measure multiple vegetation variables for field validation of remote sensing data. Calibration of remote sensing data is often performed either by coarse visual estimation or by detailed measurement in a relatively limited area (McCoy, 2005).

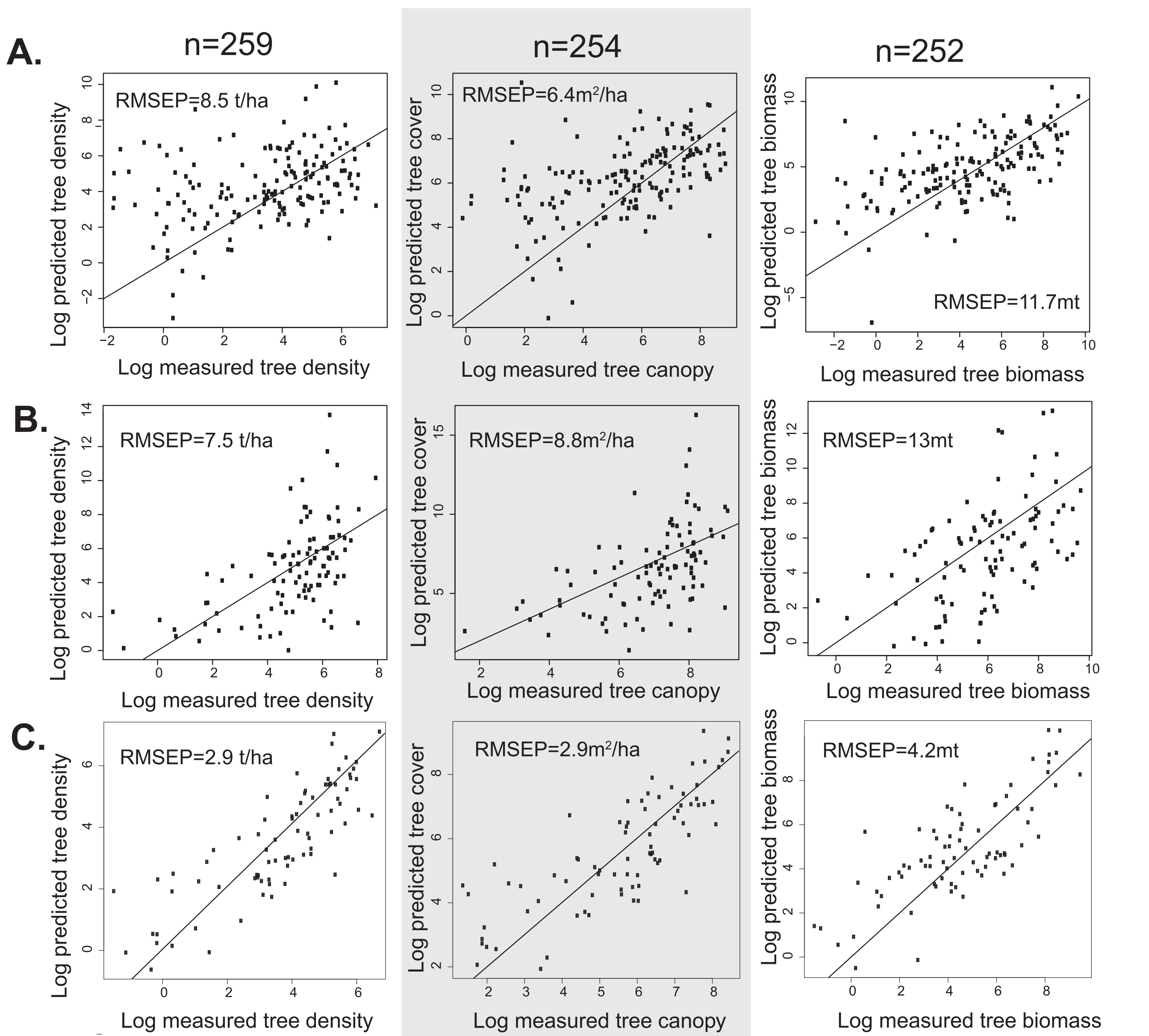

Fig. 6. Transferability of NDVI-based models for tree variables, as assessed by model predicted versus field measured log values. Diagonal lines have an aspect ratio of 1. A. Transferability in space: from wet to dry areas. B. Transferability in space: from dry to wet areas. C. Transferability in time: from 2011 to 2012. t/ha = trees per hectare; mt – metric tons.

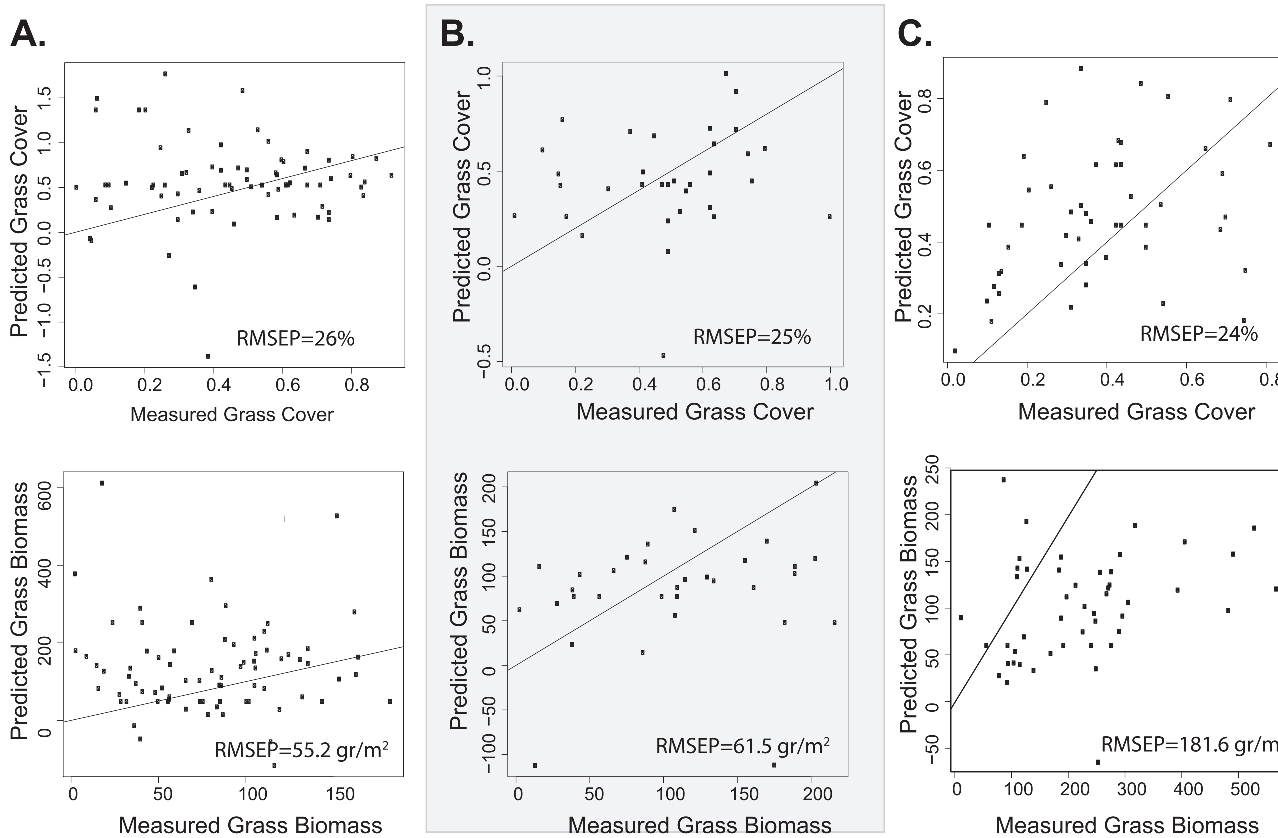

Fig. 7. Transferability of FPAR-based models for grass variables, as assessed by model predicted versus field measured log values. Diagonal lines have an aspect ratio of 1. n = 83. A. Transferability in space: from wet to dry areas. B. Transferability in space: from dry to wet areas. C. Transferability in time: from 2011 to 2012. Upper panel shows grass cover (percent cover); lower panel shows grass biomass (g/m^2).

Here we combine visual estimation with detailed measurement of vegetation variables over large area and multiple sampling points. The point centered quarter (PCQ) method we use to measure woody vegetation proves to be a rapid and efficient technique for collecting large amount of data points. Indeed, PCQ has been suggested to be a good method that combines accuracy and efficiency (Engeman et al., 1994).

Our extensive field sampling methodology enabled us to use remote sensing to predict three key vegetation variables: density, cover, and biomass. While these variables are somewhat correlated, they are not identical. Each of these variables has complementary ecological importance, and contributes unique information to the overall understanding of the vegetation community structure (Abdallah et al., 2016; Tsalyuk and Getz 2015; Vander Yacht et al., 2016). Moreover, we sampled three different vegetation forms: grass, shrubs, and trees. Each of these vegetation forms has a different ecosystem function; for example, in distribution of grazing versus browsing wildlife, fire intensity (Alleaume

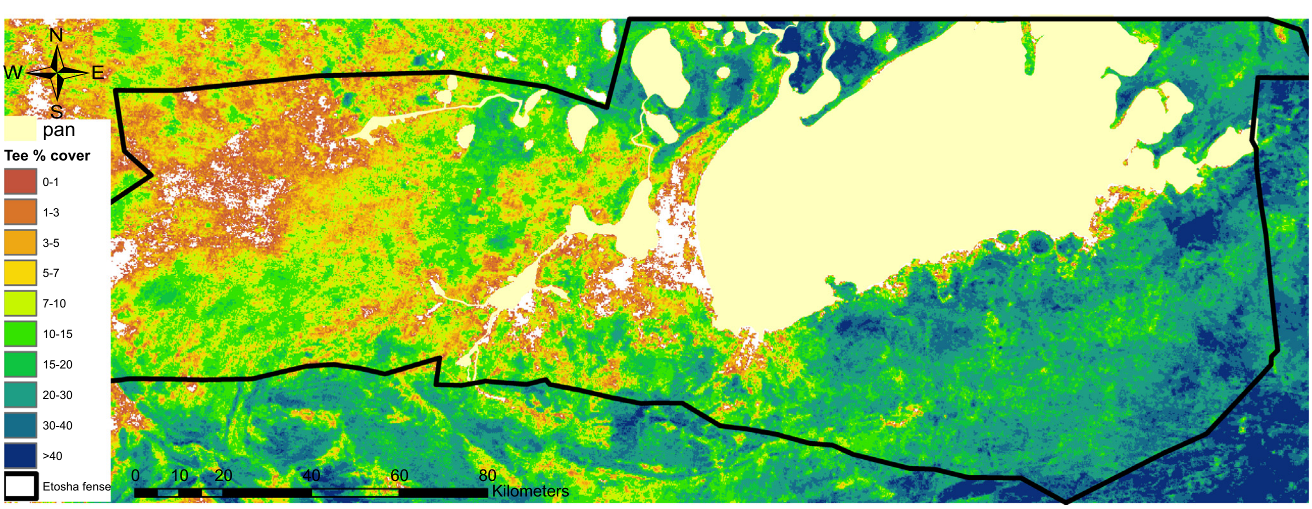

Fig. 8. Percent tree canopy cover in Etosha National park as predicted by NDVI PLSR model.

et al., 2005; Sow et al., 2013), protection of soil, and water retention. Therefore, the ability of our methodology to predict all three vegetation forms adds a valuable remote sensing-based tool for savanna vegetation monitoring.

There was difference in the ability of different MODIS-based models to predict vegetation variables. Models predicted all tree measurements and shrub density and cover well, with high explained variance and low error (Table 5). During the dry season, shrubs and trees are clearly distinct from the surrounding grass and soil by maintaining some moisture and photosynthetic activity, and therefore can be better detected by remote sensing. Conversely, while models for grass cover and biomass gave high prediction (high R^2 values), they exhibited high error (Table 4); possibly due to large variation in grass cover in different parts of Etosha and to limited ability to measure understory grass.

4.2. Time series data

Predictive models based on summary statistics of one year of VP data perform much better than a model based on only a single closest-date value. This coincides with a large body of research that has demonstrated that integrated or annual maximum VI values allow better mapping of biomass and cover, of both woody and herbaceous vegetation (Gaughan et al., 2013; Sannier et al., 2002; Zhang et al., 2016; Zhou et al., 2013). Here, we further demonstrate that including time series data of up to six years significantly improves ability to predict vegetation variables. Individual dates of VP values had large coefficients in the prediction models, indicating that fine scale temporal VP information improves model predictive ability, beyond the annually averaged data. Interestingly, the maximum annual VP values had important role in the prediction (Fig. 5). Indeed, previous research has shown that transition dates in vegetation phenological cycle can be useful in MODIS-based vegetation monitoring (Hmimina et al., 2013; Lu et al., 2014a, 2014b; Zhang et al., 2003).

We show that VP values from two or three years prior to the time of field measurement had large coefficients in the prediction model (Fig. 5). This might indicate a lag in vegetation response to previous climate conditions, which further confirms the importance of using time series in predictive vegetation models. In arid environments water availability, which is determined by mean annual rainfall, constrains vegetation cover (Sankaran et al., 2005). Dry savannas respond rapidly to rainfall event and produce a signal that can be captured by remote sensing (Schmidt and Karnieli, 2000). However, current biomass is also determined by the relative fraction of herbaceous and woody cover and by the distribution of moisture in the soil (D'Odorico et al., 2007; Knoop and Walker, 1985). Therefore, how vegetation growth responds to rainfall varies between years, which results in a multiannual lag between rainfall and the resulting biomass (Goward and Prince, 1995). Integrating remote sensing information over few years incorporates these variations, hence providing a better prediction of vegetation cover and biomass (Scanlon et al., 2005). Overall, our results demonstrate that time series of MODIS data can significantly improve model prediction of vegetation variables.

4.3. Predictive power of MODIS-derived vegetation products

We demonstrate that the four MODIS-based Vegetation Products (VPs) have complementary ability to predict different field vegetation variables. EVI produced the best model of grass and shrub cover, NDVI was the best predictor of tree density and cover, while FPAR was the best predictor of biomass (Tables 4–6). However, the differences between the VPs were rather small.

We demonstrate good prediction ability of NDVI-based models for all vegetation forms (R^2 = 75–84%), coinciding with previous literature (Li et al., 2015a; Zhang et al., 2016; Zhu and Liu, 2015). However, for grass and shrub vegetation other VPs exceeded NDVI's performance. As expected, EVI was a good predictor of savanna vegetation cover. EVI incorporates reduction in soil background and aerosol scattering, which particularly constitute a challenge in sparse vegetation cover (Jin et al., 2013; Sjostrom et al., 2011). EVI has been previously demonstrated to provide land cover information at a broad scale (Zhang Xia et al., 2008).

FPAR was the best predictor of tree biomass (1–4% higher R^2 than other VPs), and predicted grass biomass 7% better than EVI, with 10% lower error than the model using NDVI (Table 4). Although these differences of FPAR to the other VP-based models are not very high, we believe MODIS-FPAR has a strong potential to predict vegetation variables in savannas. FPAR may be superior predictor of vegetation biomass because while NDVI/EVI are good measures of green vegetation, FPAR measures structural and functional properties of vegetation, which are more relevant to senesced vegetation prevalent in savanna ecosystems (Knyazikhin et al., 1999; Myneni et al., 2002). FPAR measures the photosynthetic activity of vegetation, which continues, to some extent, in dry vegetation as well (Butterfield and Malmstrom, 2009). Indeed, previous research demonstrated that FPAR has a strong relationship with both green and senescent grassland biomass (Malmstrom, et al. 2009; Tsalyuk, et al. 2015).

The MODIS algorithm for FPAR includes the red and infrared wavelengths, the same as used in NDVI. In addition, MODIS FPAR uses information on the local biome and canopy structure, to create an accurate relationship between NDVI and the vegetation properties at each location, with extensive ground validation (Knyazikhin et al., 1999). These additional data sets may improve the correlation between FPAR and the ground-based measurements of vegetation (Fensholt et al., 2004). Indeed, since MODIS-FPAR captures leaf structure and photosynthetic activity, it was demonstrated to correlate well with seasonal ecosystem productivity in Australian tropical savanna (Restrepo-Coupe et al., 2015). FPAR is an important vegetation structural measures that are often collected in the field (Baret and Guyot, 1991). In this paper, we demonstrate the ability of satellite-based FPAR to improve prediction of savanna vegetation, beyond the traditional use of NDVI. Improvements to the MODIS LAI/FPAR model in Collection 6 (MOD15A2H) may enhance the advantage of this product even further by increasing its accuracy and resolution (Yan et al., 2016).

MODIS FPAR and LAI have higher temporal resolution than MODIS NDVI and EVI, while the latter have finer spatial resolution. MODIS FPAR and LAI are calculated as an 8-day composite measure, while NDVI and EVI are calculated for every 16-days. The finer temporal resolution of FPAR may encompass fine-scale variability in the vegetation and therefore provide better prediction of field measurements. Nonetheless, temporal composition of vegetation indices over longer periods may produce better prediction of vegetation measurements by removing angular effects and using minimum aerosol contamination (Yi et al., 2008; Zhou et al., 2013). MODIS NDVI/EVI have a finer spatial resolution of 250×250 m while MODIS FPAR and LAI are calculated for 1×1 km pixels. Coarser spatial resolution may increase vegetation prediction accuracy at a regional scale (Li et al., 2015a). Conversely, higher spatial resolution can detect fine scale spatial heterogeneity in vegetation variables. Our results demonstrate that each vegetation type is best predicted by another MODIS vegetation product, in spite of the differences in the products' spatial and temporal scales. Therefore, it is recommended that choice of vegetation product to use should be based on the vegetation variable in interest, while the imagery resolution should be dictated by the specific management need: a higher spatial resolution is necessary for small regions with high spatial heterogeneity, while higher temporal resolution is needed for regions with rapid environmental change (Boschetti et al., 2013; Dube and Mutanga, 2015; Li et al., 2015a, 2015b; Lu et al., 2014a; Zhou et al., 2013).

4.4. Transferability

One of the primary challenges in using remote sensing for vegetation prediction in semiarid environments is transferability, the ability to use models created in one place for vegetation prediction in another (Cutler et al., 2012; Eisfelder et al., 2012; Lu, 2006; Wenger and Olden, 2012). Different regions or times may have different probability distribution of the data, different variance, and, importantly, value ranges that extend beyond the data range of the model. Here we address the challenge of transferability between areas with different environmental conditions and between seasons.

Foody et al. (2003) identified the necessary components to produce a transferable remote sensing model: accurate field data, clean remote sensing information, and a region-specific relationship between biophysical information and reflectance data. Our work supports their general rule. We achieved a good spatial transferability of shrub and tree models, with good correlation between predicted and measured data and low error. We were able to achieve these results because of extensive field validation combined with high dimensionality remote sensing data. PLSR models are able to use extensive information, which encompasses most variability of field measurement, while reducing collinearity in the data by creating new orthogonal latent variables (Mevik and Wehrens, 2007). The successful transferability suggests that we were able to produce robust predictive model without overfitting the data (Darvishzadeh et al., 2011; Foody et al., 2003).

Interestingly, transferring a model created in a drier area to predict vegetation in wetter areas provided better predictions than the reverse. In drier areas, the reflectance contrasts and the differences in greening periods among the savanna vegetation forms (grass, shrubs, and trees) are more pronounced, allowing better predictions of each form. A robust predictive model created in drier areas identifies the critical changing points of a narrower phenology cycle (Archibald and Scholes, 2007), and therefore may produce better prediction for wetter areas as well (Cutler et al., 2012; Foody et al., 2003). This suggests that it might be advisable to use a training dataset from areas with a lower precipitation gradient when calibrating remote sensing-based models.

The relationship between remote sensing reflectance data and field vegetation variables depends on canopy structure and coverage (Schoettker et al., 2010). The MODIS LAI/FPAR products are based on a radiance transfer model calibrated specifically for each biome (Yan et al., 2016). Our results show that FPAR indeed improves model transferability for a wider range of data, as long it is within the same global biome.

A promising result we show here is the ability to use remote sensing models built for one year to predict vegetation variables in another. This has important practical implications for applying remote sensing-based models to monitoring vegetation change in savannas. To apply this method to quantify change over time, it should be further investigated whether or not temporal transferability can be applied in areas with larger variations in vegetation conditions.

5. Conclusions

In this paper, we have presented a rapid, low cost methodology for assessing savanna vegetation, using freely available and preprocessed MODIS satellite data. We showed that comparing few MODIS-derived Vegetation Products over time can produce reliable and robust models to predict a large suite of vegetation variables. Additionally, we demonstrate the ability of MODIS-based FPAR to predict vegetation biomass of all vegetation forms. Furthermore, we demonstrated reasonable model transferability across space and time. Based on our results, we created full cover maps for the density, cover, and biomass of grasses, shrubs, and trees for Etosha National Park (e.g. Fig. 8). These maps can be used to further understand key ecological processes in savanna ecosystems, such as spatial patterns of Gross Primary Productivity (GPP), carbon sequestration, fire load prediction, and soil and vegetation degradation processes. Applying our approach to other large savanna landscapes, will allow researchers to use freely available, high quality remote sensing products, to manage and conserve ecosystems that provide livelihood to hundreds of millions of people and preserve the rich biodiversity upon which crucial ecosystems services depend.

Acknowledgements

We thank the Namibian Ministry of Environment and Tourism (MET) for the permission to conduct fieldwork, and for providing facilities and resources for this work. We are grateful to the staff at the Etosha Ecological Institute (EEI) for scientific and technical assistance, particularly Werner Killian, Shayne Kötting, Wilferd Versfeld, Marthin Kasaona, Birgit Kötting, Ndapanda Kanime, and Erastus Ithana. We thank Etosha's wardens and rangers, and the staff of Namibia Wildlife Resorts (NWR) in Etosha. Emilia Haimbili and Maria Johannes provided dedicated assistance in fieldwork. Audrey Taylor, Janelle Dorcy, Ashley Poggio, Angie Pettenato, and Jake Toy helped in data digitizing. The National Herbarium of Namibia performed excellent work identifying species samples. The Geospatial Innovation Facility (GIF) at the University of California, Berkeley provided state of the art facilities and geospatial support. Professor Maureen Lahiff provided statistical assistance.

Funding

This research was funded by the Science and Engineering fellowship from the Center for Emerging and Neglected diseases (CEND); Andrew and Mary Thomson Rocca dissertation research fellowship; and NIH Grant GM083863 and a USFWS Grant to WMG. Sponsors did not have any role in the study design, collection, analysis and interpretation of data, writing of the report, nor in the decision to submit this article for publication.

Appendix A. Supplementary material

Supplementary data associated with this article can be found, in the online version, at http://dx.doi.org/10.1016/j.isprsjprs.2017.07.012.

References

Abdallah, F., Michalet, R., Maalouf, J., Ouled-Dhaou, S., Touzard, B., Noumi, Z., et al., 2016. Disentangling canopy and soil effects of a savanna tree species on its understorey. J. Veg. Sci. 27 (4), 771–779.
Ali, I., Cawkwell, F., Dwyer, E., Barrett, B., Green, S., 2016. Satellite remote sensing of grasslands: from observation to management—a review. J. Plant Ecol. rtw005.
Alleaume, S., Hely, C., Le Roux, J., Korontzi, S., Swap, R.J., Shugart, H.H., et al., 2005. Using MODIS to evaluate heterogeneity of biomass burning in southern African savannahs: a case study in Etosha. Int. J. Remote Sens. 26 (19), 4219–4237.
Archibald, S., Scholes, R.J., 2007. Leaf green-up in a semi-arid African savanna – separating tree and grass responses to environmental cues. J. Veg. Sci. 18 (4), 583–594.
Asner, G.P., Wessman, C.A., Archer, S., 1998. Scale dependence of absorption of photosynthetically active radiation in terrestrial ecosystems. Ecol. Appl. 8 (4), 1003–1021.
Asner, G.P., Martin, R.E., 2008. Spectral and chemical analysis of tropical forests: scaling from leaf to canopy levels. Remote Sens. Environ. 112 (10), 3958–3970.

Ban, Y., Gong, P., Gini, C., 2015. Global land cover mapping using Earth observation satellite data: recent progresses and challenges. ISPRS J. Photogr. Rem. Sens. 103, 1–6.
Baret, F., Guyot, G., 1991. Potentials and limits of vegetation indexes for Lai and Apar assessment. Remote Sens. Environ. 35 (2–3), 161–173.
Boschetti, M., Nutini, F., Brivio, P.A., Bartholome, E., Stroppiana, D., Hoscilo, A., 2013. Identification of environmental anomaly hot spots in West Africa from time series of NDVI and rainfall. ISPRS J. Photogr. Rem. Sens. 78, 26–40.
Butterfield, H.S., Malmstrom, C.M., 2009. The effects of phenology on indirect measures of aboveground biomass in annual grasses. Int. J. Remote Sens. 30 (11/12), 3133–3146.
Choudhury, B., 1992. Multispectral satellite-observations for arid land studies. ISPRS J. Photogr. Rem. Sens. 47 (2–3), 101–126.
Ciais, P., Bombelli, A., Williams, M., Piao, S.L., Chave, J., Ryan, C.M., et al., 2011. The carbon balance of Africa: synthesis of recent research studies. Philos. Trans. R. Soc. A – Math. Phys. Eng. Sci. 369 (1943), 2038–2057.
Cutler, M., Boyd, D., Foody, G., Vetrivel, A., 2012. Estimating tropical forest biomass with a combination of SAR image texture and Landsat TM data: an assessment of predictions between regions. ISPRS J. Photogr. Rem. Sens. 70, 66–77.
Darvishzadeh, R., Atzberger, C., Skidmore, A., Schlerf, M., 2011. Mapping grassland leaf area index with airborne hyperspectral imagery: a comparison study of statistical approaches and inversion of radiative transfer models. ISPRS J. Photogr. Rem. Sens. 66 (6), 894–906.
Darvishzadeh, R., Skidmore, A., Schlerf, M., Atzberger, C., Corsi, F., Cho, M., 2008. LAI and chlorophyll estimation for a heterogeneous grassland using hyperspectral measurements. ISPRS J. Photogr. Rem. Sens. 63 (4), 409–426.
de Beer, Y., Kilian, W., Versfeld, W., van Aarde, R.J., 2006. Elephants and low rainfall alter woody vegetation in Etosha National Park, Namibia. J. Arid Environ. 64 (3), 412–421.
D'Odorico, P., Caylor, K., Okin, G.S., Scanlon, T.M., 2007. On soil moisture–vegetation feedbacks and their possible effects on the dynamics of dryland ecosystems. J. Geophys. Res.: Biogeosci. 112 (G4).
Du Plessis, W.P., 1999. Linear regression relationships between NDVI, vegetation and rainfall in Etosha National Park, Namibia. J. Arid Environ. 42 (4), 235–260.
Du Plessis, W.P., 2001. Effective rainfall defined using measurements of grass growth in the Etosha National Park Namibia. J. Arid Environ. 48 (3), 397–417.
Du Plessis, W.P., Bredenkamp, G.J., Trollope, W.S.W., 1998. Response of herbaceous species to a degradation gradient in the western region of Etosha National Park, Namibia. Koedoe 41 (1), 9–18.
Dube, T., Mutanga, O., 2015. Evaluating the utility of the medium-spatial resolution Landsat 8 multispectral sensor in quantifying aboveground biomass in uMgeni catchment, South Africa. ISPRS J. Photogr. Rem. Sens. 101, 36–46.
Eisfelder, C., Kuenzer, C., Dech, S., 2012. Derivation of biomass information for semi-arid areas using remote-sensing data. Int. J. Remote Sens. 33 (9), 2937–2984.
Engeman, R.M., Sugihara, R.T., Pank, L.F., Dusenberry, W.E., 1994. A comparison of plotless density estimators using Monte-Carlo simulation. Ecology 75 (6), 1769–1779.
EODIS, 2013. Earth Observing System Data and Information System. Earth Observing System Clearing House (ECHO)/Reverb. <http://reverb.echo.nasa.gov/>.
ESRI, 2011. ArcGIS Deskto: Release 10.2.
Fensholt, R., Sandholt, I., Rasmussen, M., 2004. Evaluation of MODIS LAI, fAPAR and the relation between fAPAR and NDVI in a semi-arid environment using in situ measurements. Remote Sens. Environ. 91 (3–4), 490–507.
Foody, G.M., Boyd, D.S., Cutler, M.E.J., 2003. Predictive relations of tropical forest biomass from Landsat TM data and their transferability between regions. Remote Sens. Environ. 85 (4), 463–474.
Gaughan, A.E., Holdo, R.M., Anderson, T.M., 2013. Using short-term MODIS time-series to quantify tree cover in a highly heterogeneous African savanna. Int. J. Remote Sens. 34 (19), 6865–6882.
Geladi, P., Kowalski, B.R., 1986. Partial least-squares regression: a tutorial. Anal. Chim. Acta 185, 1–17.
Ghulam, A., Qin, Q., Teyip, T., Li, Z., 2007. Modified perpendicular drought index (MPDI): a real-time drought monitoring method. ISPRS J. Photogr. Rem. Sens. 62 (2), 150–164.
Goward, S., Prince, S., 1995. Transient effects of climate on vegetation dynamics: satellite observations. J. Biogeogr. 22 (2–3), 549–564.
Hansen, P.M., Schjoerring, J.K., 2003. Reflectance measurement of canopy biomass and nitrogen status in wheat crops using normalized difference vegetation indices and partial least squares regression. Remote Sens. Environ. 86 (4), 542–553.
Henry, M., Picard, N., Trotta, C., Manlay, R.J., Valentini, R., Bernoux, M., et al., 2011. Estimating tree biomass of Sub-Saharan African forests: a review of available allometric equations. Silva Fennica 45 (3), 477–569.
Hmimina, G., Dufrene, E., Pontailler, J., Delpierre, N., Aubinet, M., Caquet, B., et al., 2013. Evaluation of the potential of MODIS satellite data to predict vegetation phenology in different biomes: an investigation using ground-based NDVI measurements. Remote Sens. Environ. 132, 145–158.
Homer, C.G., Meyer, D.K., Aldridge, C.L., Schell, S.J., 2013. Detecting annual and seasonal changes in a sagebrush ecosystem with remote sensing-derived continuous fields. J. Appl. Remote Sens. 7 (1). 073508–073508.
Houborg, R., Soegaard, H., Boegh, E., 2007. Combining vegetation index and model inversion methods for the extraction of key vegetation biophysical parameters using Terra and Aqua MODIS reflectance data. Remote Sens. Environ. 106 (1), 39–58.
Huang, Z., Turner, B.J., Dury, S.J., Wallis, I.R., Foley, W.J., 2004. Estimating foliage nitrogen concentration from HYMAP data using continuum removal analysis. Remote Sens. Environ. 93 (1–2), 18–29.
Huete, A., Didan, K., Miura, T., Rodriguez, E.P., Gao, X., Ferreira, L.G., 2002. Overview of the radiometric and biophysical performance of the MODIS vegetation indices. Remote Sens. Environ. 83 (1–2), 195–213.
Huete, A.R., 1988. A Soil-Adjusted Vegetation Index (Savi). Remote Sens. Environ. 25 (3), 295–309.
Jacquin, A., Sheeren, D., Lacombe, J., 2010. Vegetation cover degradation assessment in Madagascar savanna based on trend analysis of MODIS NDVI time series. Int. J. Appl. Earth Obs. Geoinf. 12, S3–S10.
Jin, C., Xiao, X., Merbold, L., Arneth, A., Veenendaal, E., Kutsch, W.L., 2013. Phenology and gross primary production of two dominant savanna woodland ecosystems in Southern Africa. Remote Sens. Environ. 135, 189–201.
Knoop, W., Walker, B., 1985. Interactions of woody and herbaceous vegetation in a southern African savanna. J. Ecol., 235–253
Knyazikhin, Y., Glassy, J., Privette, J.L., Tian, Y., Lotsch, A., Zhang, Y., et al., 1999. MODIS Leaf Area Index (LAI) and Fraction of Photosynthetically Active Radiation Absorbed by Vegetation (FPAR) Product (MOD15) Algorithm Theoretical Basis Document.
Knyazikhin, Y., Martonchik, J.V., Myneni, R.B., Diner, D.J., Running, S.W., 1998. Synergistic algorithm for estimating vegetation canopy leaf area index and fraction of absorbed photosynthetically active radiation from MODIS and MISR data. J. Geophys. Res. – Atmos. 103 (D24), 32257–32275.
Lazaridis, D.C., Verbesselt, J., Robinson, A.P., 2011. Penalized regression techniques for prediction: a case study for predicting tree mortality using remotely sensed vegetation indices. Can. J. For. Res. – Revue Canadienne De Recherche Forestiere 41 (1), 24–34.
Li, S., Potter, C., Hiatt, C., 2012. Monitoring of net primary production in California rangelands using Landsat and MODIS satellite remote sensing. Nat. Resour. 3 (2), 56–65.
Li, L., Guo, Q., Tao, S., Kelly, M., Xu, G., 2015a. Lidar with multi-temporal MODIS provide a means to upscale predictions of forest biomass. ISPRS J. Photogr. Rem. Sens. 102, 198–208.
Li, Q., Wang, C., Zhang, B., Lu, L., 2015b. Object-based crop classification with Landsat-MODIS enhanced time-series data. Rem. Sensing 7 (12), 16091–16107.
Le Roux, C.J.G., Grunow, J.O., Morris, J.W., Bredenkamp, G.J., Scheepers, J.C., 1988. A Classification of the Vegetation of the Etosha National Park South-West Africa. South African J. Bot. 54 (1), 1–10.
Lotsch, A., Tian, Y., Friedl, M.A., Myneni, R.B., 2003. Land cover mapping in support of LAI and FPAR retrievals from EOS-MODIS and MISR: classification methods and sensitivities to errors. Int. J. Remote Sens. 24 (10), 1997–2016.
LP DAAC, 2002–2012. The Land Processes Distributed Active Archive Center. NASA Land Processes Distributed Active Archive Center. MCD15A2. <https://lpdaac.usgs.gov/data_access>.
Lu, D.S., 2006. The potential and challenge of remote sensing-based biomass estimation. Int. J. Remote Sens. 27 (7), 1297–1328.
Lu, L., Kuenzer, C., Guo, H., Li, Q., Long, T., Li, X., 2014a. A novel land cover classification map based on a MODIS time-series in Xinjiang, China. Rem. Sensing 6 (4), 3387–3408.
Lu, L., Wang, C., Guo, H., Li, Q., 2014b. Detecting winter wheat phenology with SPOT-VEGETATION data in the North China Plain. Geocarto Int. 29 (3), 244–255.
Machwitz, M., Gessner, U., Conrad, C., Falk, U., Richters, J., Dech, S., 2015. Modelling the gross primary productivity of West Africa with the regional biomass model RBM, using optimized 250 m MODIS FPAR and fractional vegetation cover information. Int. J. Appl. Earth Obs. Geoinf. 43, 177–194.
Malmstrom, C.M., Butterfield, H.S., Barber, C., Dieter, B., Harrison, R., Qi, J., et al., 2009. Using remote sensing to evaluate the influence of grassland restoration activities on ecosystem forage provisioning services. Restor. Ecol. 17 (4), 526–538.
Mathieu, R., Wessels, K., Asner, G., Knapp, D., van Aardt, J., Main, R., et al., 2009. Tree cover, tree height and bare soil cover differences along a land use degradation gradient in semi-arid savannas, South Africa. 2009 IEEE International Geoscience and Remote Sensing Symposium, vols. 1–5, pp. 445–448.
Mayr, M.J., Samimi, C., 2015. Comparing the dry season in-situ Leaf Area Index (LAI) derived from high-resolution RapidEye imagery with MODIS LAI in a Namibian Savanna. Rem. Sensing 7 (4), 4834–4857.
McCoy, R.M., 2005. Field Methods in Remote Sensing. Anonymous Guilford Press, pp. 71–88.
Mevik, B.H., Cederkvist, H.R., 2004. Mean squared error of prediction (MSEP) estimates for principal component regression (PCR) and partial least squares regression (PLSR). J. Chemom. 18 (9), 422–429.
Mevik, B., Wehrens, R., 2007. The pls package: principal component and partial least squares regression in R. J. Stat. Softw. 18 (2), 1–23.
Meyer, T., Okin, G., 2015. Evaluation of spectral unmixing techniques using MODIS in a structurally complex savanna environment for retrieval of green vegetation, nonphotosynthetic vegetation, and soil fractional cover. Remote Sens. Environ. 161, 122–130.
Mitchard, E.T.A., Flintrop, C.M., 2013. Woody encroachment and forest degradation in sub-Saharan Africa's woodlands and savannas 1982–2006. Philos. Trans. R. Soc. B – Biol. Sci. 368 (1625), 20120406.
Mitchell, J.J., Glenn, N.F., Sankey, T.T., Derryberry, D.R., Germino, M.J., 2012. Remote sensing of sagebrush canopy nitrogen. Remote Sens. Environ. 124, 217–223.
Myneni, R., Knyazikhin, Y., Shabanov, N., 2010. Leaf area index and fraction of absorbed PAR products from Terra and Aqua MODIS sensors: analysis,

validation, and refinement. In: Land Remote Sensing and Global Environmental Change. Anonymous Springer, pp. 603–633.
Myneni, R.B., Hoffman, S., Knyazikhin, Y., Privette, J.L., Glassy, J., Tian, Y., et al., 2002. Global products of vegetation leaf area and fraction absorbed PAR from year one of MODIS data. Remote Sens. Environ. 83 (1–2), 214–231.
Naidoo, L., Cho, M.A., Mathieu, R., Asner, G., 2012. Classification of savanna tree species, in the Greater Kruger National Park region, by integrating hyperspectral and LiDAR data in a Random Forest data mining environment. ISPRS J. Photogr. Rem. Sens. 69, 167–179.
Pollard, J.H., 1971. Distance estimators of density in randomly distributed forests. Biometrics 27 (4), 991.
Qiu, B., Luo, Y., Tang, Z., Chen, C., Lu, D., Huang, H., et al., 2017. Winter wheat mapping combining variations before and after estimated heading dates. ISPRS J. Photogr. Rem. Sens. 123, 35–46.
Rahimzadeh-Bajgiran, P., Omasa, K., Shimizu, Y., 2012. Comparative evaluation of the Vegetation Dryness Index (VDI), the Temperature Vegetation Dryness Index (TVDI) and the improved TVDI (iTVDI) for water stress detection in semi-arid regions of Iran. ISPRS J. Photogr. Rem. Sens. 68, 1–12.
Ramoelo, A., Skidmore, A.K., Cho, M.A., Mathieu, R., Heitkonig, I.M.A., Dudeni-Tlhone, N., et al., 2013. Non-linear partial least square regression increases the estimation accuracy of grass nitrogen and phosphorus using in situ hyperspectral and environmental data. ISPRS J. Photogr. Rem. Sens. 82, 27–40.
Rao, Y., Zhu, X., Chen, J., Wang, J., 2015. An improved method for producing high spatial-resolution NDVI time series datasets with multi-temporal MODIS NDVI data and Landsat TM/ETM plus images. Rem. Sensing 7 (6), 7865–7891.
Restrepo-Coupe, N., Huete, A., Davies, K., Cleverly, J., Beringer, J., Eamus, D., et al., 2015. MODIS vegetation products as proxies of photosynthetic potential: a look across meteorological and biologic driven ecosystem productivity. Biogeosci. Discuss. 12 (23).
Sankaran, M., Hanan, N.P., Scholes, R.J., Ratnam, J., Augustine, D.J., Cade, B.S., et al., 2005. Determinants of woody cover in African savannas. Nature 438 (7069), 846–849.
Sankaran, M., Augustine, D.J., Ratnam, J., 2013. Native ungulates of diverse body sizes collectively regulate long-term woody plant demography and structure of a semi-arid savanna. J. Ecol. 101 (6), 1389–1399.
Sannier, C.A.D., Taylor, J.C., Du Plessis, W., CAmpbell, K., 1996. Application of remote sensing and GIS for monitoring vegetation in Etosha National Park. In: Rosenberg, L.J., Power, C.H., Downey, I. (Eds.), Remote Sensing and GIS for Natural Resource Management. Natural Resources Institute, Chatham, UK, pp. 101–106.
Sannier, C.A.D., Taylor, J.C., Du Plessis, W., 2002. Real-time monitoring of vegetation biomass with NOAA-AVHRR in Etosha National Park, Namibia, for fire risk assessment. Int. J. Remote Sens. 23 (1), 71–89.
Scanlon, T.M., Caylor, K.K., Manfreda, S., Levin, S.A., Rodriguez-Iturbe, I., 2005. Dynamic response of grass cover to rainfall variability: implications for the function and persistence of savanna ecosystems. Adv. Water Resour. 28 (3), 291–302.
Schmidt, H., Karnieli, A., 2000. Remote sensing of the seasonal variability of vegetation in a semi-arid environment. J. Arid Environ. 45 (1), 43–59.
Schmidtlein, S., Sassin, J., 2004. Mapping of continuous floristic gradients in grasslands using hyperspectral imagery. Remote Sens. Environ. 92 (1), 126–138.
Schoettker, B., Scarth, P., Phinn, S., Denham, R., Schmidt, M., 2010. Estimation of vegetation parameters from MODIS FPAR time series, Landsat TM and ETM+ products, and ICESat for soil erosion modelling. In: Proceedings 2010 IEEE International Geoscience and Remote Sensing Symposium (IGARSS 2010), pp. 2083–2086.
Shackleton, C.M., Scholes, R.J., 2011. Above ground woody community attributes, biomass and carbon stocks along a rainfall gradient in the savannas of the central lowveld, South Africa. S. Afr. J. Bot. 77 (1), 184–192.
Sjostrom, M., Ardo, J., Arneth, A., Boulain, N., Cappelaere, B., Eklundh, L., et al., 2011. Exploring the potential of MODIS EVI for modeling gross primary production across African ecosystems. Remote Sens. Environ. 115 (4), 1081–1089.
Solano, R., Didan, K., Jacobson, A., Huete, A., 2010. MODIS Vegetation Index User's Guide (MOD13 Series). pp. 1–38.
Solbrig, O.T., 1996. The diversity of the savanna ecosystem. In: Biodiversity and Savanna Ecosystem Processes. Anonymous Springer, pp. 1–27.
Song, K., Li, L., Tedesco, L.P., Li, S., Duan, H., Liu, D., et al., 2013. Remote estimation of chlorophyll-a in turbid inland waters: three-band model versus GA-PLS model. Remote Sens. Environ. 136, 342–357.
Sow, M., Mbow, C., Hely, C., Fensholt, R., Sambou, B., 2013. Estimation of herbaceous fuel moisture content using vegetation indices and land surface temperature from MODIS data. Rem. Sensing 5 (6), 2617–2638.
Sumnall, M., Peduzzi, A., Fox, T.R., Wynne, R.H., Thomas, V.A., Cook, B., 2016. Assessing the transferability of statistical predictive models for leaf area index between two airborne discrete return LiDAR sensor designs within multiple intensely managed Loblolly pine forest locations in the south-eastern USA. Remote Sens. Environ. 176, 308–319.
Svoray, T., Perevolotsky, A., Atkinson, P.M., 2013. Ecological sustainability in rangelands: the contribution of remote sensing. Int. J. Remote Sens. 34 (17), 6216–6242.
Taylor, J.C., Bird, A.C., Sannier, C., Pratt, N., Plessis, W.d., 1996. Calibration and validation of thematic maps from remote sensing in Developing Countries: need and method. Remote sensing and GIS for natural resource management, 39–46.
Trollope, W., Potgieter, A., 1986. Estimating grass fuel loads with a disc pasture meter in the Kruger National Park. J. Grassland Soc. S. Afr. 3 (4), 148–152.
Tsalyuk, M., Kelly, M., Koy, K., Getz, W.M., Butterfield, H.S., 2015. Monitoring the impact of grazing on rangeland conservation easements using MODIS vegetation indices. Rangeland Ecol. Manage. 68 (2), 173–185.
Tsalyuk, M., Getz, M.W., 2015. The effect of ambient environmental cues and individual state on resource selection in african elephants. In: International Conference for Conservation Biology, Anonymous Montpellier, France.
Tucker, C.J., Holben, B.N., Elgin, J.H., Mcmurtrey, J.E., 1981. Remote-sensing of total dry-matter accumulation in winter-wheat. Remote Sens. Environ. 11 (3), 171–189.
Vågen, T., Lal, R., Singh, B., 2005. Soil carbon sequestration in sub-Saharan Africa: a review. Land Degrad. Dev. 16 (1), 53–71.
van Hoek, M., Jia, L., Zhou, J., Zheng, C., Menenti, M., 2016. Early drought detection by spectral analysis of satellite time series of precipitation and normalized difference vegetation index (NDVI). Rem. Sensing 8 (5), 422.
Vander Yacht, A.L., Keyser, P.D., Buehler, D.A., Harper, C.A., Buckley, D.S., Applegate, R.D., 2016. Avian occupancy response to oak woodland and savanna restoration. J. Wildlife Manage. 80 (6), 1091–1105.
Verbesselt, J., Somers, B., van Aardt, J., Jonckheere, I., Coppin, P., 2006. Monitoring herbaceous biomass and water content with SPOT VEGETATION time-series to improve fire risk assessment in savanna ecosystems. Remote Sens. Environ. 101 (3), 399–414.
Vogel, M., Strohbach, M., 2009. Monitoring of savanna degradation in Namibia using Landsat TM/ETM+ data. In: 2009 IEEE International Geoscience and Remote Sensing Symposium (IGARSS 2009), pp. 931–934.
Warde, W., Petranka, J.W., 1981. A correction factor table for missing point-center quarter data. Ecology 62 (2), 491–494.
Weiss, D.J., Atkinson, P.M., Bhatt, S., Mappin, B., Hay, S.I., Gething, P.W., 2014. An effective approach for gap-filling continental scale remotely sensed time-series. ISPRS J. Photogr. Rem. Sens. 98, 106–118.
Wenger, S.J., Olden, J.D., 2012. Assessing transferability of ecological models: an underappreciated aspect of statistical validation. Methods Ecol. Evol. 3 (2), 260–267.
White, N.A., Engemann, R.M., Sugihara, R.T., Krupa, H.W., 2008. A comparison of plotless density estimators using Monte Carlo simulation on totally enumerated field data sets. BMC Ecol. 8. 11 pp.–11 pp.
Wold, S., Sjöström, M., Eriksson, L., 2001. PLS-regression: a basic tool of chemometrics. Chemomet. Intellig. Lab. Syst. 58 (2), 109–130.
Xu, D., Guo, X., Li, Z., Yang, X., Yin, H., 2014. Measuring the dead component of mixed grassland with Landsat imagery. Remote Sens. Environ. 142, 33–43.
Yan, K., Park, T., Yan, G., Chen, C., Yang, B., Liu, Z., et al., 2016. Evaluation of MODIS LAI/FPAR product collection 6. Part 1: consistency and improvements. Rem. Sensing 8 (5), 359.
Yi, Y., Yang, D., Huang, J., Chen, D., 2008. Evaluation of MODIS surface reflectance products for wheat leaf area index (LAI) retrieval. ISPRS J. Photogr. Rem. Sens. 63 (6), 661–677.
Xia, Zhang, Rui, Sun, Bing, Zhang, Qingxi, Tong, 2008. Land cover classification of the North China Plain using MODIS_EVI time series. ISPRS J. Photogr. Rem. Sens. 63 (4), 476–484.
Zhang, B., Zhang, L., Xie, D., Yin, X., Liu, C., Liu, G., 2016. Application of synthetic NDVI time series blended from Landsat and MODIS data for grassland biomass estimation. Rem. Sensing 8 (1), 10.
Zhang, J., Feng, L., Yao, F., 2014. Improved maize cultivated area estimation over a large scale combining MODIS-EVI time series data and crop phenological information. ISPRS J. Photogr. Rem. Sens. 94, 102–113.
Zhang, X.Y., Friedl, M.A., Schaaf, C.B., Strahler, A.H., Hodges, J.C.F., Gao, F., et al., 2003. Monitoring vegetation phenology using MODIS. Remote Sens. Environ. 84 (3), 471–475.
Zhang, X., Zhang, Q., 2016. Monitoring interannual variation in global crop yield using long-term AVHRR and MODIS observations. ISPRS J. Photogr. Rem. Sens. 114, 191–205.
Zhao, D., Huang, L., Li, J., Qi, J., 2007. A comparative analysis of broadband and narrowband derived vegetation indices in predicting LAI and CCD of a cotton canopy. ISPRS J. Photogr. Rem. Sens. 62 (1), 25–33.
Zhou, F., Zhang, A., Townley-Smith, L., 2013. A data mining approach for evaluation of optimal time-series of MODIS data for land cover mapping at a regional level. ISPRS J. Photogr. Rem. Sens. 84, 114–129.
Zhu, X., Liu, D., 2015. Improving forest aboveground biomass estimation using seasonal Landsat NDVI time-series. ISPRS J. Photogr. Rem. Sens. 102, 222–231.